JVI Journals.ASM.org

Murine Gammaherpesvirus 68 Encoding Open Reading Frame 11 Targets TANK Binding Kinase 1 To Negatively Regulate the Host Type I Interferon Response

Hye-Ri Kang,[a] Woo-Chang Cheong,[a] Ji-Eun Park,[a] Seungbo Ryu,[a] Hye-Jeong Cho,[a] Hyunyee Youn,[a,b] Jin-Hyun Ahn,[c] Moon Jung Song[a]

Virus-Host Interactions Laboratory, Department of Biosystems and Biotechnology, Division of Biotechnology, College of Life Sciences and Biotechnology, South Korea University, Seoul, Republic of Korea[a]; Laboratory of Protein Immunology, Biomedical Research Institutes, Seoul National University Hospital, Seoul, Republic of Korea[b]; Department of Molecular Cell Biology, School of Medicine, Sungkyunkwan University, Suwon, Gueonggido, Republic of Korea[c]

ABSTRACT

Upon viral infection, type I interferons, such as alpha and beta interferon (IFN-α and IFN-β, respectively), are rapidly induced and activate multiple antiviral genes, thereby serving as the first line of host defense. Many DNA and RNA viruses counteract the host interferon system by modulating the production of IFNs. In this study, we report that murine gammaherpesvirus 68 (MHV-68), a double-stranded DNA virus, encodes open reading frame 11 (ORF11), a novel immune modulator, to block IFN-β production. ORF11-deficient recombinant viruses induced more IFN-β production in fibroblast and macrophage cells than the MHV-68 wild type or a marker rescue virus. MHV-68 ORF11 decreased IFN-β promoter activation by various factors, the signaling of which converges on TBK1-IRF3 activation. MHV-68 ORF11 directly interacted with both overexpressed and endogenous TBK1 but not with IRF3. Physical interactions between ORF11 and endogenous TBK1 were further confirmed during virus replication in fibroblasts using a recombinant virus expressing FLAG-ORF11. ORF11 efficiently reduced interaction between TBK1 and IRF3 and subsequently inhibited activation of IRF3, thereby negatively regulating IFN-β production. Our domain-mapping study showed that the central domain of ORF11 was responsible for both TBK1 binding and inhibition of IFN-β induction, while the kinase domain of TBK1 was sufficient for ORF11 binding. Taken together, these results suggest a mechanism underlying inhibition of IFN-β production by a gammaherpesvirus and highlight the importance of TBK1 in DNA virus replication.

IMPORTANCE

Gammaherpesviruses are important human pathogens, as they are associated with various kinds of tumors. Upon virus infection, the type I interferon pathway is activated by a series of signaling molecules and stimulates antiviral gene expression. To subvert such interferon antiviral responses, viruses are equipped with multiple factors that can inhibit its critical steps. In this study, we took an unbiased genomic approach using a mutant library of murine gammaherpesvirus 68 to screen a novel viral immune modulator that negatively regulates the type I interferon pathway and identified ORF11 as a strong candidate. ORF11-deficient virus infection produced more interferon than the wild type in both fibroblasts and macrophages. During virus replication, ORF11 directly bound to TBK1, a key regulatory protein in the interferon pathway, and inhibited TBK1-mediated interferon production. Our results highlight a crucial role of TBK1 in controlling DNA virus infection and a viral strategy to curtail host surveillance.

Virus infection induces various immune responses in the host which control virus replication and limit its spread. One of the earliest and most potent innate immune responses to virus infection is the transcriptional activation of type I interferons (IFNs), such as IFN-β and multiple IFN-α species. Upon secretion, all type I IFNs bind to a common IFN-α/β receptor and activate signaling through the classical Janus kinase (JAK) signal transducer and activator of transcription (STAT) pathway, which subsequently induces transcription of hundreds of IFN-stimulated genes (ISGs) with diverse antiviral responses. ISGs directly inhibit protein translation, degrade viral mRNAs, and induce apoptosis in infected cells (1–4). Indirectly, IFNs activate immune cells, such as natural killer cells and macrophages, and increase antigen presentation on the cell surface, which further limits virus propagation *in vivo* (5–8).

Type I IFN production is orchestrated by amplification of an initial wave of IFN-β that promotes expression of IFN-α. Interferon regulatory factor 3 (IRF3) and IRF7 are critical transcriptional activators for IFN production (9). In response to viral infection, cytoplasmic IRF3 becomes phosphorylated, forms dimers, and translocates into the nucleus, where it binds to CREB-binding protein (CBP)/P300 and initiates the transcription of type I IFN genes and IFN stimulatory response elements (ISREs), a consensus promoter sequence found in interferon-stimulated genes (10). IRF3 is mainly activated by two noncanonical IκB kinases, the TANK-binding kinase (TBK1; NAK or T2K) and inducible IKK (IKKi or IKKε) (9, 11–14). TBK1 and IKKε can be activated by engagement of PAMPs by the PRRs, including Toll-

Received 23 November 2014 **Accepted** 27 March 2014
Published ahead of print 2 April 2014
Editor: K. Frueh
Address correspondence to Moon Jung Song, moonsong@korea.ac.kr.

doi:10.1128/JVI.03460-13

like receptors (TLRs), cytoplasmic RIG-1-like receptors (RLRs), or cytosolic DNA sensors (15–22). Recently, the adaptor protein STING was found to play an essential role in the signaling response to cytoplasmic double-stranded DNA (dsDNA), promoting TBK1-specific activation of IRF3 (23, 24). Ubiquitously expressed TBK1 plays a critical role in type I IFN induction, particularly upon DNA virus infection, as evidenced in impairment of IFN production against DNA virus infection in TBK1$^{-/-}$ mice (25, 26). Both murine embryonic fibroblasts (MEFs) and bone marrow-derived macrophages (BMDMs) of TBK1$^{-/-}$ mice failed to produce type I IFNs against DNA virus infection, while they were able to produce normal levels of IFNs against RNA virus infection (25, 26). In contrast, BMDMs of IKKε$^{-/-}$ mice did not show any defects in production of type I IFNs against DNA virus infection, suggesting functional differences between TBK1 and IKKε in DNA virus-mediated IFN responses (25, 26).

Herpesviruses are large, double-stranded DNA viruses with the ability to persist in the host by establishing latency and by evading host immune surveillance. Two human gammaherpesviruses, Epstein-Barr virus (EBV) and Kaposi's sarcoma-associated herpesvirus (KSHV), are known as causative agents for various kinds of tumors (27, 28). Murine gammaherpesvirus 68 (MHV-68 or γHV-68) is genetically and biologically related to EBV and KSHV and is considered an important experimental system to study virus-host interactions and viral pathogenesis (29–32). MHV-68 productively replicates in epithelial and fibroblast cells and establishes latency mainly in B cells and macrophages (33–37). A whole-genome-wide library of MHV-68 mutants tagged with distinct sequences has been generated (38), which allows us to conduct a forward genetic screening for the phenotype of interest.

To successfully infect and persist in the host, herpesviruses are equipped with multiple strategies to subvert host immune responses (39). Understanding the mechanisms of how gammaherpesviruses modulate host immune responses leading to persistent infection is essential to control virus infection and their associated diseases. In this study, we sought to screen a novel viral factor that modulates the host type I IFN response using the genome-wide mutant library of MHV-68 and identified that open reading frame 11 (ORF11), the tegument protein of previously unknown function, inhibited the transactivation of the IFN-β promoter induced by various stimuli, the signaling of which converges into TBK1 and IRF3 activation. MHV-68 ORF11 directly binds to endogenous TBK1, but not to IKKε, and subsequently interferes with TBK1-IRF3 interactions, leading to efficient inhibition of IFN-β production in virus-susceptible macrophages as well as fibroblasts. Our results highlight the importance of TBK1 as a central factor in regulating the type I IFN response against DNA virus infection and a DNA viral strategy to curtail host IFN responses.

MATERIALS AND METHODS

Cells, viruses, and plaque assays. HEK293T, Raw264.7, HeLa, and Vero cells were cultured in complete Dulbecco's modified Eagle's medium containing 10% fetal bovine serum (FBS; HyClone) and supplemented with 100 U/ml penicillin and 100 μg/ml streptomycin (HyClone), while NIH 3T3 cells were cultured in 10% bovine calf serum (HyClone). MEF (murine embryonic fibroblast) cells were obtained from BALB/c and C57BL/6 mouse embryos (13.5 days) and cultured with 10% fetal bovine serum (HyClone). Bone marrow-derived macrophages (BMDMs) were cultured in RPMI 1640 medium supplemented with 10% FBS, 10 mM HEPES, 100 U/ml penicillin, 100 μg/ml streptomycin (HyClone), 50 μM beta-mercaptoethanol (Sigma), and 30% macrophage colony-stimulating factor (M-CSF) from the L929 cell line for 7 days. NIH 3T3 cells stably containing 5×ISRE-Luc (5×ISRE/NIH 3T3) were made by stably transfecting 5×ISRE-Luc plasmid and pBABE-puro (a puromycin resistance gene plasmid) at a ratio of 10:1.

MHV-68 was originally obtained from the American Type Culture Collection (ATCC VR1465). The titers of amplified or reconstituted viruses were determined by plaque assay using Vero cells overlaid with 1% methylcellulose (Sigma) in normal growth media. After 5 days of infection, the cells were fixed and stained with 2% crystal violet in 20% ethanol. Plaques were then counted to determine the titers. MHV-68 ORF11^{null} and ORF36^{null} viruses were generated by *in vitro* Mu transposition with an infectious bacterial artificial chromosome (BAC) clone of MHV-68 (pMHV-68) and purified STM transposons as described previously (38). Sendai virus (SeV) was originally obtained from Peter Palese (Icahn School of Medicine at Mount Sinai, USA) and propagated in 10-day-old embryonated eggs at 37°C for 48 h. After chilling at 4°C overnight, the titer of amplified SeV was determined using hemagglutinin assays. The viruses were stored in aliquots at −70°C until use.

Plasmids and molecular cloning. MHV-68 ORF11 wild-type (WT) and domain mutant constructs were prepared in pENTR vector of the Gateway system (Invitrogen) using the following primers: ORF11 WT (F, 5′-TCGACTGGATCCATGGCGGAGAGTCACCC-3′; R, 5′-AGATATCTCGAGTTTGAAACAGTTGGGGA-3′), ORF11 ΔΔC1(1–195) (F, 5′-CCGGAATTCATGGCGGAGAGTCACCCATGG-3′; R, 5′-ATAAGAATGCGGCCGCTCAGACGGCTGTGAAGACGC-3′), ORF11 ΔC2(1–288) (F, 5′-CCGGAATTCATGGCGGAGAGTCACCCATGG-3′; R, 5′-ATAAGAATGCGGCCGCTCAAATACTGATGGTTTCCAGCGG-3′), ORF11 ΔN1(196–388) (F, 5′-CCGGAATTCATGTTTCCCGGGCTCCACAGG −3′; R, 5′-ATAAGAATGCCGGCCGCTCATTTGAAACAGTTGGGGAGGG-3′), ORF11 ΔN2(85–388) (F, 5′-CCGGAATTCATGGGCCTGCTCCTGTTTGG-3′; R, 5′-ATAAGAATGCGGCCGCTCATTTGAAACAGTTGGGGAGGG-3′), and ORF11 CD(85–288) (F, 5′-CCGGAATTCATGTTTCCCGGGCTCCACAGG-3′; R, 5′-ATAAGAATGCGGCCGCTCAAATACTGATGGTTTCCAGCGG-3′). The entry clones were further transferred to FLAG-tagging (pTAG-attR-C1) and hemagglutinin (HA)-tagging (pSG5-HA) destination vectors according to the manufacturer's instructions. In particular, Myc-tagged (pCS3-MT-6-Myc) ORF11 was generated using a modified version of the pCS-MT plasmid as a destination vector containing the 6× Myc tag with additional sequences. For construction of ORF11-expressed lentiviral vector, an amplified ORF11 PCR product was cloned into pCMV2-FLAG using primers 5′-GGATAAGCTTGCAGCTGCAATGGCGGAGAGTCACCCATGG-3′ (F) and 5′-GTGTAGGATCCTTATTTGAAACAGTTGGGGAG-3′ (R) and then subcloned into modified lentiviral pCDH-MCS-T2A-copGFP-MSCV vector (CD523A-1; System Biosciences, Mountain View, CA) (40) using primers 5′-GCCAATATAGCTAGCACCATGGACTACAAAGAC-3′ (F) and 5′-GCTCTATGCGGCCGCTTTGAAACAGTTGGGGAGGG-3′ (R). IFI16 (from Andrew Bowie, Trinity College Dublin, Ireland), STING, TBK1, TBK1 K38A, IKKε (from Kate Fitzgerald, University of Massachusetts Medical School, USA), RIG-I, TRIF (from Joo-Young Lee, Gwang-Ju Institute of Science and Technology, Republic of Korea), IRF3, IRF3-5D, IFN-β-Luc, 5×ISRE-Luc, and MAVS (from Ren Sun and Genhong Cheng, University of California, Los Angeles, CA) plasmids were prepared by following a standard protocol (Qiagen). Inserts for TBK1 domain mutants were amplified with the following primers and cloned into pCDNA-FLAG: TBK1 KD/ULD (F, 5′-GTGTAGGATCCGCCACCATGGACTACAAG-3′; R, 5′-GCCTCTAGACTAGCTTACTACAAATATAGG-3′) and TBK1 KD (F, 5′-GTGTAGGATCCGCCACCATGGACTACAAG-3′; R, 5′-GCCTCTAGACTATTCTGCAAAAAACTGG-3′).

Generation of 11ST, 11ST/MR, and FLAG-ORF11/MHV-68 viruses. To generate an ORF11-deficient recombinant MHV-68 clone, a shuttle plasmid based on pGS284 (kindly provided by Greg Smith, Northwestern University, USA) was constructed. The translational stop codons at the ORF11 locus were introduced by a two-step PCR approach. The sequences upstream (nucleotides [nt] 23228 to 23688) of the stop codons were amplified by primers 11AF (F, 5′-tat*agatct*ttcaccaagtctgtggctac-3′)

and 11AR (F, 5′-cagatcatactggaagacgcTAACTGAGT*aagcttgcggccgc*gggc-3′), and the downstream sequences (nt 23681 to 24121) were amplified by primers 11BF (F, 5′-acgcTAACTGAGT*aagcttgcggccgc*gggcaccgtggggtccgc cc-3′) and 11BR (F, 5′-att*gctagc*caaatcccataaaatttagg-3′). The uppercase letters indicate the stop codon sequences, and italic letters indicate the restriction enzyme sites containing BglII, HindIII, NotI, and NheI sites. In a subsequent PCR, two PCR products were mixed as templates and amplified with primers of AF and BR. The final PCR products were cloned into pGS285 using BglII and NheI sites (pGS284-11ST). The WT sequences of ORF11 were amplified with primers of AF and BR using bacterial artificial chromosome (BAC) DNA of MHV-68 as a template and cloned into pGS284 to generate a marker rescue virus (11ST/MR). The recombinant MHV-68 BAC plasmids of 11ST and 11ST/MR were generated by the two-step allelic exchange method (41, 42). Insertion or removal of stop codons was screened by PCR and restriction enzyme digestion and confirmed by sequencing. The genome integrity of positive clones was further examined by restriction enzyme digestion and Southern blot analysis. A BAC plasmid of 11ST or 11ST/MR was reconstituted in BHK21 cells by cotransfecting a Cre recombinase-expressing plasmid using Lipofectamine Plus (Invitrogen) to excise the BAC sequences. The genome integrity of the produced viruses was determined by restriction enzyme digestion and Southern analysis, and their titers were measured by plaque assays. To generate a FLAG-ORF11/MHV-68 virus, we produced PCR constructs containing 3×FLAG coding sequence on an inducible I-SceI and kanamycin-resistant gene cassette. 3×FLAG coding sequences were inserted between nt 24651 and nt 24652 (tagggataacagggtaat tgatagggataacagggtaat*accgcc*ATGGACTACAAAGACCATGACGGT GATTATAAAGATCATGACATCGATTACAAGGATGACGATGA CAAGtga). The uppercase letters indicate the FLAG coding sequence, the italic letters indicate the Kozak sequence, and the lowercase letters indicate the viral genome sequence. The recombinant MHV-68 BAC plasmids of FLAG-ORF11/MHV-68 were generated by a two-step red-mediated recombination method (43). The genome integrity of positive clones was examined by restriction enzyme digestion.

Southern blot analysis. BAC plasmids of MHV-68 WT, 11ST, and 11ST/MR were incubated with EcoRI and NotI. Digested DNA was loaded into 0.7% agarose gel and transferred to a nylon membrane (Amersham Biosciences). The probe was a PCR product (nt 23228 to 24121) amplified with primers ORF11 AF and ORF11 BR and generated by a random priming method with [α-^{32}P]dCTP. Radioactivity was detected and analyzed by using a multiplex bioimaging system (FLA-7000; Fujifilm).

Multiple growth curves of viruses. The replication kinetics of the WT, 11ST, and 11ST/MR viruses were assayed in NIH 3T3 and MEF cells. The cells were incubated with viral inocula for 1 h at an MOI of 0.05. After 1 h of incubation, the inocula were removed, and the cells were washed three times with phosphate-buffered saline (PBS) and added to fresh medium. The cells and the supernatants were harvested together at various time points and subjected to three rounds of freezing and thawing. The virus titers of the supernatants were analyzed by plaque assays.

Transfection and transduction. Polyethylenimine (1 mg/ml) (Sigma) was used for 293T cell transfection, while Lipofectamine Plus (Invitrogen) and Lipofectamine 2000 (Invitrogen) were used according to the manufacturer's instructions for Vero cells and NIH 3T3 cell transfection, respectively. To produce the lentivirus, a modified lentiviral vector (from pCDH-MCS-T2A-copGFPMSCV; System Biosciences) was used to clone FLAG-ORF11 (40). The ORF11-expressing lentiviral vector (pCDH-MCS-T2A-copGFPMSCV-ORF11) and packaging vectors (pMD2.G and pspA-X2) were cotransfected into HEK293T cells. Supernatants were harvested every 12 h after the transfection and changed to complete media for 3 days. The supernatants were incubated with Raw264.7 cells and changed every 24 h for 3 days for transduction. The lentivirus-transduced cells expressing green fluorescent protein (GFP) were sorted by a FACSAria (BD Bioscience).

Luciferase reporter assays. The luciferase reporter assay system (Promega) was used to measure promoter activity. The cell lysates were washed with 1× PBS and incubated with 100 μl of passive lysis buffer (10% glycerol, 1% Triton X-100, 2 mM EDTA, 2 mM dithiothreitol [DTT], and 24 mM Tris-HCl [pH 7.8]). Lysates were frozen, thawed once, and centrifuged at top speed in a centrifuge for 5 min. In all assays, firefly luciferase activity from the reporters was normalized with β-galactosidase (β-gal), GFP, or *renilla*.

ELISA. Cells were infected with MHV-68 or SeV at the indicated MOI, and the supernatants were harvested at the indicated time points. Released amounts of IFN-β were measured by IFN-β enzyme-linked immunosorbent assay (ELISA) kits (PBL) according to the manufacturer's instructions.

Quantitative real-time PCR (RT-qPCR). For quantification of cellular transcripts, total RNA was extracted using Tri Reagent (MRC) and chloroform extraction methods. The cDNAs were synthesized using a RevertAid first-strand cDNA synthesis (Fermentas, South Korea) with random hexamers. Transcripts were quantified by using IFN-β primers (F, 5′-AAACTCATGACCAGTCTGCA-3′; R, 5′-AGGAGATCTTCAGT TTCGGAGC-3′) and normalized by actin primers (F, 5′-GTATCCTGA CCCTGAAGTACC-3′; R, 5′-TGAAGGTCTCAAACATGATCT-3′). The experiment was performed on an iCycler iQ multicolor real-time PCR detection system and analyzed on Optical system software (Bio-Rad). Reverse-transcribed cDNAs were mixed with a homemade mix. SYBR green PCR was run at 95°C for 15 min and 45 cycles of 95°C for 30 s, 55°C for 30 s, and 72°C for 30 s, followed by melting curve analysis. All quantitative PCRs were performed and analyzed in an iCycler iQ (Bio-Rad).

Coimmunoprecipitation and antibodies. HEK293T cells were seeded, transfected with the indicated plasmids, and incubated for 48 h. Cells were scraped and resuspended in the immunoprecipitation (IP) buffer (20 mM HEPES, pH 7.4, 100 mM NaCl, 0.5% Nonidet P-40, and 1% Triton X-100) supplemented with a 1/100 volume of protease inhibitor cocktail (Sigma). Cells were rotated at 4°C for 1 h, and cell debris was removed by centrifugation (12,000 rpm, 4°C, 10 min). Appropriate antibodies were added, and lysates were incubated at 4°C with rotating. After that, 30 μl protein A/G agarose beads (Pierce) was added and further incubated at 4°C. The beads were washed extensively by IP buffer, and proteins were analyzed by Western blot analysis. The samples were probed with primary antibodies to FLAG-M2 (1:2,000; Sigma), GFP (1:500; Santa Cruz), HA (1:300; Santa Cruz), Myc-c-horseradish peroxidase (HRP) (1:5,000; Roche), phospho-IRF3 (Ser396) (1:200; Cell Signaling), TBK1 (1:100; Cell Signaling), and tubulin (1:2,000; Sigma). Goat anti-rabbit or goat anti-mouse immunoglobulin G conjugated with horseradish peroxide secondary antibody (Santa Cruz) was detected by ECL plus Western blot detection reagents (ELPIS), and the signals were detected and analyzed using LAS-4000, a chemiluminescent image analyzer (Fujifilm).

Immunofluorescence assay (IFA) and confocal microscopy. HEK293T cells were seeded on the cover glass of a 24-well plate. On the following day, 293T cells were transfected with the indicated plasmids. After 24 h, cells were fixed with 4% paraformaldehyde and 0.15% picric acid in PBS. A blocking step was performed with 10% normal goat serum and 0.3% Triton X-100 in 0.1% bovine serum albumin (BSA) containing 1× PBS. For staining, anti-FLAG-M2 (Sigma), anti-HA probe (Santa Cruz), and anti-TBK1 (Abcam) were used as a first antibody for 12 h at 4°C, and rabbit-IgG was used as a control antibody. Mouse-Cy3, rabbit-Cy3, and mouse-FITC (Jackson ImmunoResearch) were used as secondary antibodies for 45 min at room temperature. DAPI stain (1:1,000) was used for nuclear staining for 3 min at room temperature. Thereafter, cover glass was mounted onto slide glass using a Shandon Immu-Mount (Thermo Scientific). The stained cells were visualized at ×1,000 magnification under a confocal laser scanning microscope (LSM 5 Exciter; Zeiss).

RESULTS

Identification of a viral factor that regulates the host type I IFN response. To screen a viral factor that counteracts the host antiviral IFN response during MHV-68 replication, we generated an IFN-β reporter cell line harboring the 5×ISRE-Luc reporter plasmid in NIH 3T3 cells (5×ISRE/3T3), which were activated by

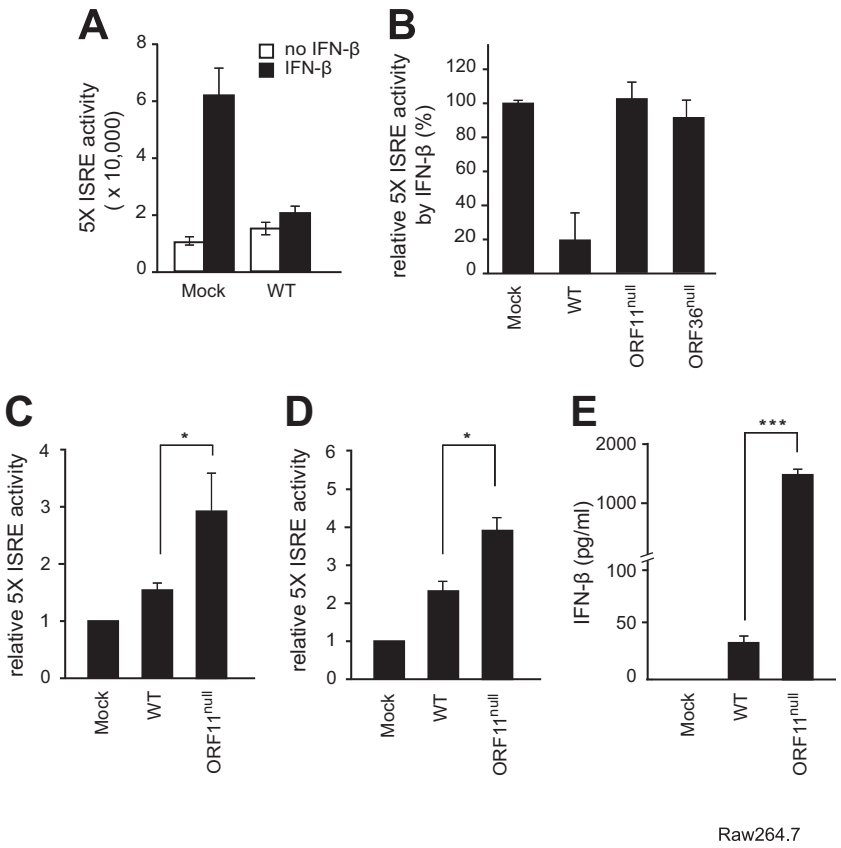

FIG 1 Identification of ORF11 as a viral immune modulator that downregulates the IFN-β signaling pathway. (A) MHV-68 infection downregulated ISRE activation induced by IFN-β treatment. NIH 3T3 cells harboring the 5×ISRE-Luc reporter plasmid (5×ISRE/3T3) were mock infected or infected with MHV-68 for 30 to 32 h (MOI, 1) and treated with mouse IFN-β (500 U/ml) for 6 to 8 h. The harvested cell lysates were analyzed for luciferase activities. The results were from three independent experiments, and standard deviations are shown. (B) Screening of replication-competent MHV-68 mutants in 5×ISRE/3T3 cells. Replication-competent MHV-68 mutants were individually infected in 5×ISRE/3T3 cells for 30 to 36 h (MOI, 1), and then mouse IFN-β (500 U/ml) was supplied for 6 to 8 h. At least three independent experiments were performed for individual viruses, and relative activities of 5×ISRE-Luc were calculated with the 5×ISRE activity of mock infection set as 100% for each experiment. Results with WT, ORF11^{null}, and ORF36^{null} viruses are shown as representative results from our screenings. (C and D) ORF11^{null} virus infection elevated the levels of IFN-β produced in fibroblasts and macrophages upon infection. MEFs (C) and Raw264.7 cells (D) were infected with WT or ORF11^{null} virus at an MOI of 2 for 6 h. The supernatants were transferred to 5×ISRE/3T3 cells and incubated for an additional 12 h, and relative 5×ISRE activity was measured and compared to that of mock infection ($n = 3$). (E) Raw264.7 cells were infected with WT or ORF11^{null} virus at an MOI of 2 for 12 h. IFN-β amounts in the supernatants were measured by ELISA. Each error bar shows the means ± standard deviations. *, $P < 0.05$ (Student's *t* test).

IFN-β treatment in a dose-dependent manner (data not shown). The 5×ISRE/3T3 reporter cells were infected with MHV-68 at an MOI of 1 for 30 to 32 h, followed by IFN-β treatment (500 U/ml) for 6 to 8 h. MHV-68 infection decreased transactivation of 5×ISRE-Luc induced by IFN-β treatment compared to mock infection, suggesting that MHV-68 expresses viral factors that block the IFN-β signaling and/or production upon virus infection (Fig. 1A). To systematically identify such a viral factor antagonizing the host IFN response, we took advantage of our genome-wide replication-competent MHV-68 mutant library (38) and screened for a mutant that reversed the WT phenotype in 5×ISRE/3T3 cells following IFN-β treatment (500 U/ml). We found that ORF36-deficient virus (ORF36^{null}) infection did not lower 5×ISRE-Luc activation (Fig. 1B). ORF36, a conserved herpesviral kinase, was previously reported to inhibit IRF3-mediated type I IFN-β production (44), validating our screening system. We also found that ORF11-deficient virus (ORF11^{null}) infection failed to decrease the IFN-β-induced 5×ISRE activity (Fig. 1B).

MHV-68 ORF11 is classified as an early-late gene (45–47) and is associated with virions (48). Although ORF11 was dispensable for viral growth *in vitro* (38, 48), ORF11 deficiency led to attenuation in lytic replication *in vivo* and delayed seeding to the spleen for latency (48). However, the function of MHV-68 ORF11 is unknown. To further examine whether ORF11 can interfere with type I IFN-β production similarly to ORF36, we infected the WT or ORF11^{null} virus into murine embryonic fibroblasts (MEFs) and Raw264.7 macrophage cells at an MOI of 2 for 24 h and measured the relative activity of released IFN-β by transferring the supernatants from the infected cells into 5×ISRE/3T3 cells (Fig. 1C and D). ORF11^{null} virus infection in macrophages and MEFs induced significantly higher levels of IFN-β than the WT virus, as shown in higher 5×ISRE activity of transferred supernatants. Consistent with this, a higher level of IFN-β protein was detected in ORF11^{null} infection than in WT infection according to ELISA (Fig. 1E). In summary, our screening system newly identified ORF11 with a previously unknown function as a viral immune modulator that may inhibit IFN-β production in both fibroblasts and macrophages during virus infection.

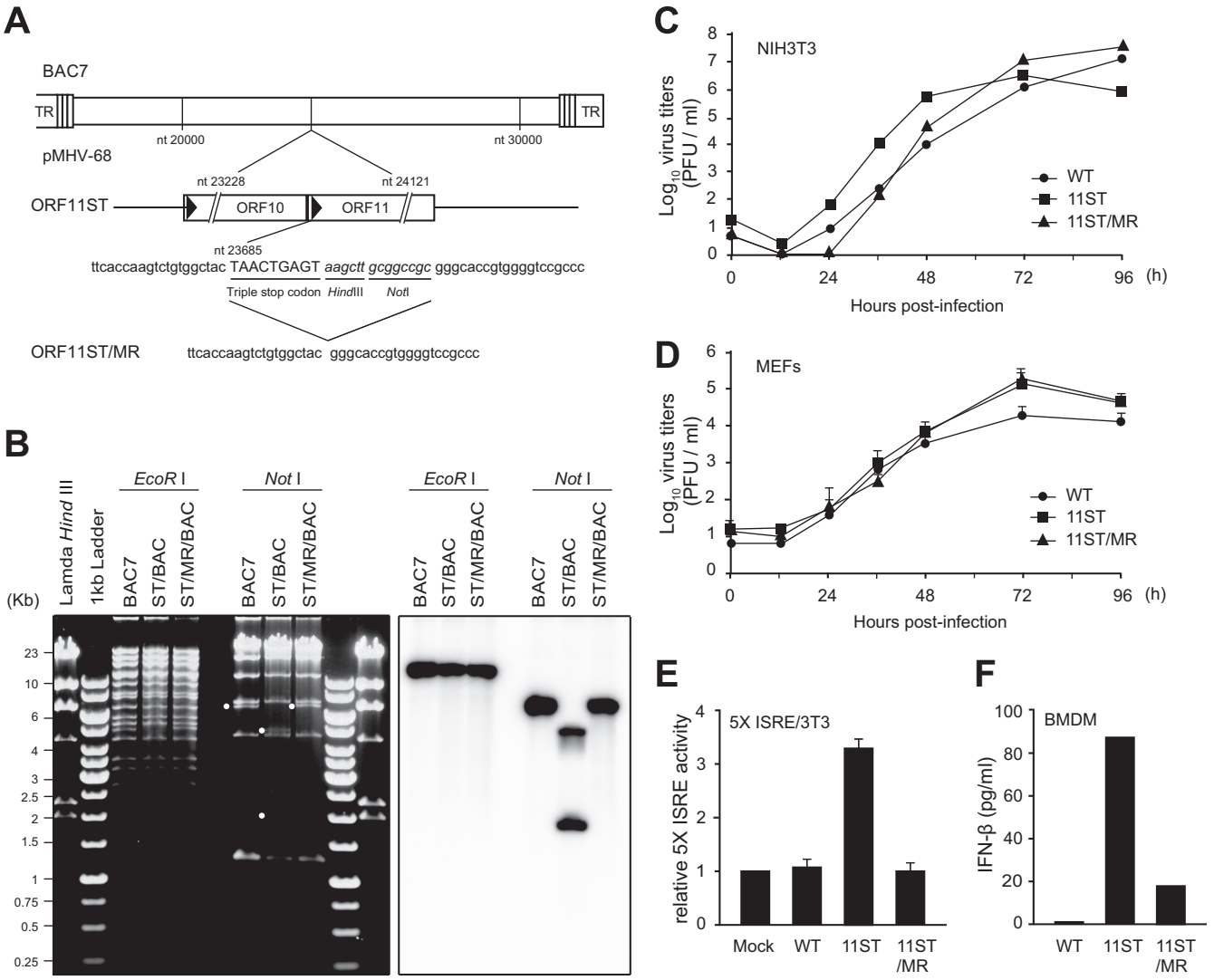

FIG 2 Infection of MHV-68 lacking ORF11 induces the IFN-β signaling pathway. (A) Schematic diagram of the ORF11 locus in the MHV-68 genome. (B) Construction of the 11ST and 11ST marker rescue (11ST/MR) viruses. Stop codons were introduced into the ORF11 locus (nt 23685) using two-step allelic exchange in the MHV-68 BAC clone. BAC DNAs for the wild type, 11ST, and 11ST/MR viruses were digested by EcoRI and NotI, resolved in 0.7% agarose gel, and subjected to Southern blot analysis using a ^{32}P-labeled ORF11-specific probe. (C and D) Virus growth of the WT, 11ST, and 11ST/MR viruses in fibroblasts. NIH 3T3 (C) and MEFs (D) were infected with WT, 11ST, or 11ST/MR virus at an MOI of 0.05 and harvested at the indicated time points. The virus titers in the cells and the supernatants were analyzed by plaque assays. (E and F) 11ST virus infection resulted in increased production of IFN-β in fibroblasts and macrophages upon infection. (E) The 5×ISRE-Luc reporter cells were infected with WT, 11S, and 11S/MR viruses (MOI, 2), and relative 5×ISRE activity was measured at 24 h postinfection and compared to that of mock infection. (F) BMDMs were infected with WT, 11S, and 11S/MR viruses (MOI, 2) for 8 h, and the amounts of IFN-β in the supernatants were measured by ELISA. Error bars show the means ± standard deviations.

ORF11 deficiency affected the host type I IFN response in fibroblasts and macrophages. ORF11^{null} harbors a 1.2-kb-long transposon which may affect neighboring gene functions. To confirm that the phenotype of ORF11^{null} was due to disrupted ORF11 expression, another ORF11-deficient virus (11ST) containing triple stop codons at the ORF11 locus (nt 23685) and its marker rescue revertant (11ST/MR) were generated using the allelic exchange method (Fig. 2A). The viral genome integrities of 11ST and 11ST/MR were confirmed by restriction enzyme mapping and Southern blotting (Fig. 2B). Consistent with previous reports (38, 48), multiple-step growth curves of the 11ST virus showed no replication defect in NIH 3T3 and MEF cells (Fig. 2C and D). However, 11ST infection induced higher ISRE activation in 5×ISRE/3T3 cells and elevated levels of IFN-β protein in bone marrow-derived macrophages (BMDMs) than WT or 11ST/MR infection (Fig. 2E and F). These results confirm our previous results that ORF11 deficiency increased the host type I IFN response in fibroblasts and macrophages.

ORF11 inhibits IFN-β promoter activity. Infection of ORF11-deficient viruses into fibroblasts and macrophages led to elevated levels of IFN-β (Fig. 1C to E and 2E and F). To confirm the function and understand the mechanisms of ORF11 in negatively regulating IFN-β production, we examined the effects of ORF11 on transactivation of the IFN-β promoter by various stimuli. Sendai virus (SeV) is known to elicit strong IFN-β responses in a RIG-I-dependent manner (49). When HEK293T cells were infected with

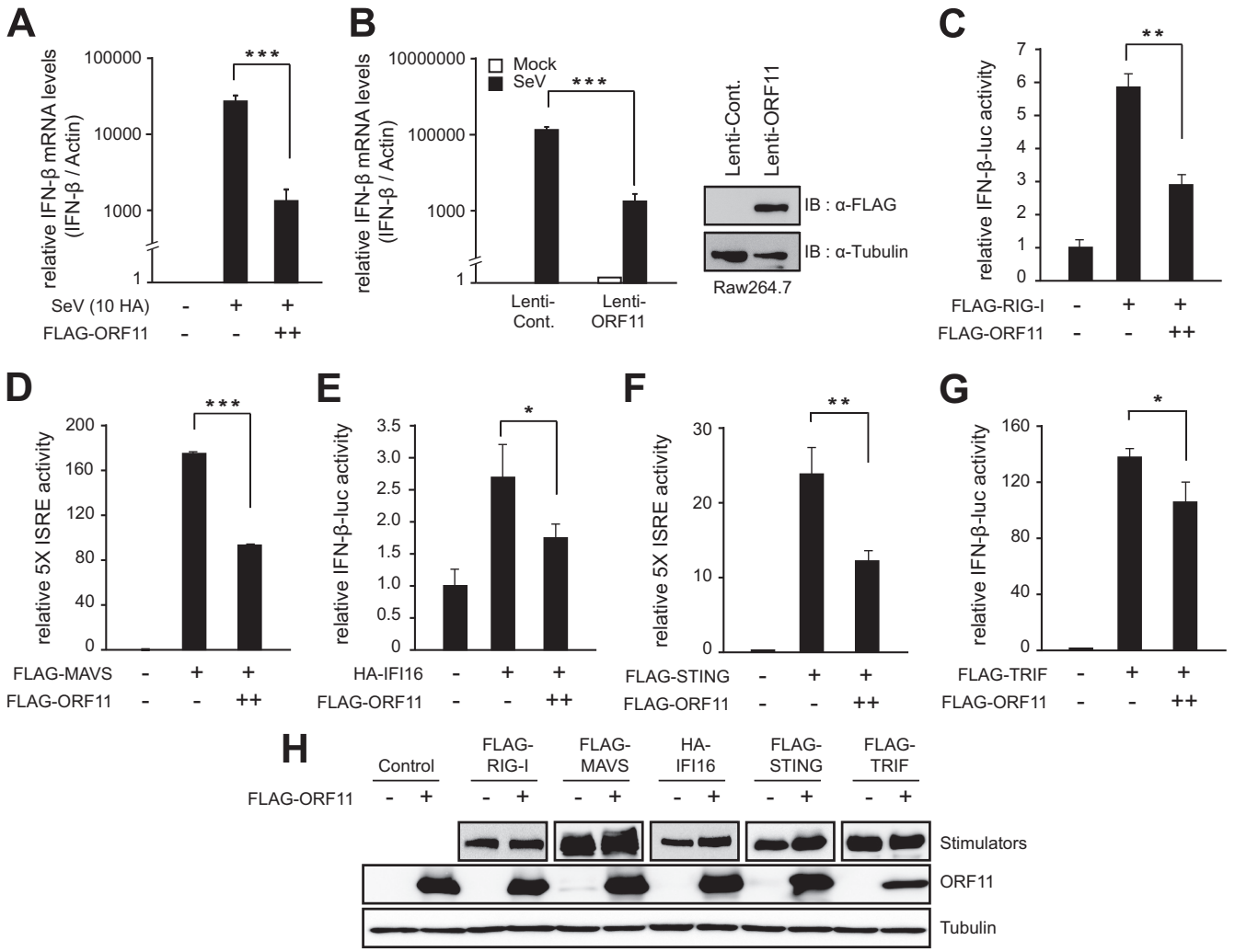

FIG 3 MHV-68 ORF11 inhibits the IFN-β production and promoter activity. (A) MHV-68 ORF11 decreased the level of the IFN-β transcripts upon Sendai virus (SeV) infection in fibroblasts. HEK293T cells were transiently transfected with a vector alone or FLAG-ORF11 for 24 h and infected with SeV (10 HA units). After 18 h postinfection, the total RNA was extracted and relative *Ifnb* mRNA levels were measured and normalized to actin mRNA levels by RT-qPCR. (B) ORF11 ablated SeV-induced IFN-β mRNA levels in macrophages. Raw264.7 cells stably expressing a control vector (Lenti-Cont.) or FLAG-ORF11 (Lenti-ORF11) were generated by lentiviral transduction and infected with SeV (10 HA units) for 18 h. Relative *Ifnb* mRNA levels were analyzed as mentioned for panel A. The expression of ORF11 was shown in the transduced cells using Western blot analysis with anti-FLAG (right). IB, immunoblot. (C and G) FLAG-ORF11 inhibited IFN-β promoter activity. Vector alone or FLAG-OF11 (400 ng) was transiently cotransfected into HEK293T cells with RIG-I (500 ng; C), MAVS (20 ng; D), IFI16 (400 ng; E), STING (50 ng; F), or TRIF (50 ng; G). The cells were harvested at 24 h posttransfection and subjected to luciferase reporter assays. The β-gal (C, E, and G) or *renilla* luciferase activities (D and F) were used as a control. (H) HEK293T cells were cotransfected with various expression vectors in the presence or absence of ORF11, harvested at 24 h posttransfection, and analyzed by Western blotting. The data are shown as means ± standard deviations. *, $P < 0.05$; **, $P < 0.01$; ***, $P < 0.001$ (Student's *t* test).

SeV following transient transfection with FLAG-ORF11, the endogenous *Ifnb* mRNA was significantly decreased compared to that of the vector control (Fig. 3A). To test whether ORF11 function can be recapitulated in macrophages, we established a Raw264.7 cell line stably expressing ORF11 by transducing a FLAG-ORF11 lentivirus (Fig. 3B, right) and found that the endogenous *Ifnb* mRNA was significantly decreased in ORF11-expressing macrophages upon SeV infection (Fig. 3B). ORF11 expression reduced transactivation of the IFN promoter (IFN-β-Luc) induced by RIG-I in HEK293T cells (Fig. 3C). Similarly, ORF11 decreased IFN-β-Luc activated by MAVS, a downstream adaptor of RIG-I (Fig. 3D). ORF11 also reduced the IFN promoter activity induced by IFI16, a cytoplasmic DNA sensor (Fig. 3E). STING, a downstream adaptor of cytosolic DNA sensors, was also tested, and the results indicated that ORF11 downregulated STING-mediated activity (Fig. 3F). When TRIF, an adaptor protein inducing IFN-β from TLRs, stimulated the IFN-β-Luc transactivation, ORF11 overexpression reduced its activation to a lesser extent (Fig. 3G). The expression levels of these stimulators remained similar even in the presence of ORF11, suggesting that ORF11 does not directly affect the stability of these molecules (Fig. 3H). Although some stimulators, such as RIG-I and TRIF, can also activate the interferon promoter in a TBK1-independent manner, these stimuli are known to commonly activate TBK1-IRF3 for type I interferon production. Therefore, our results led us to hypothesize that ORF11 targets TBK1-IRF3 activation during virus

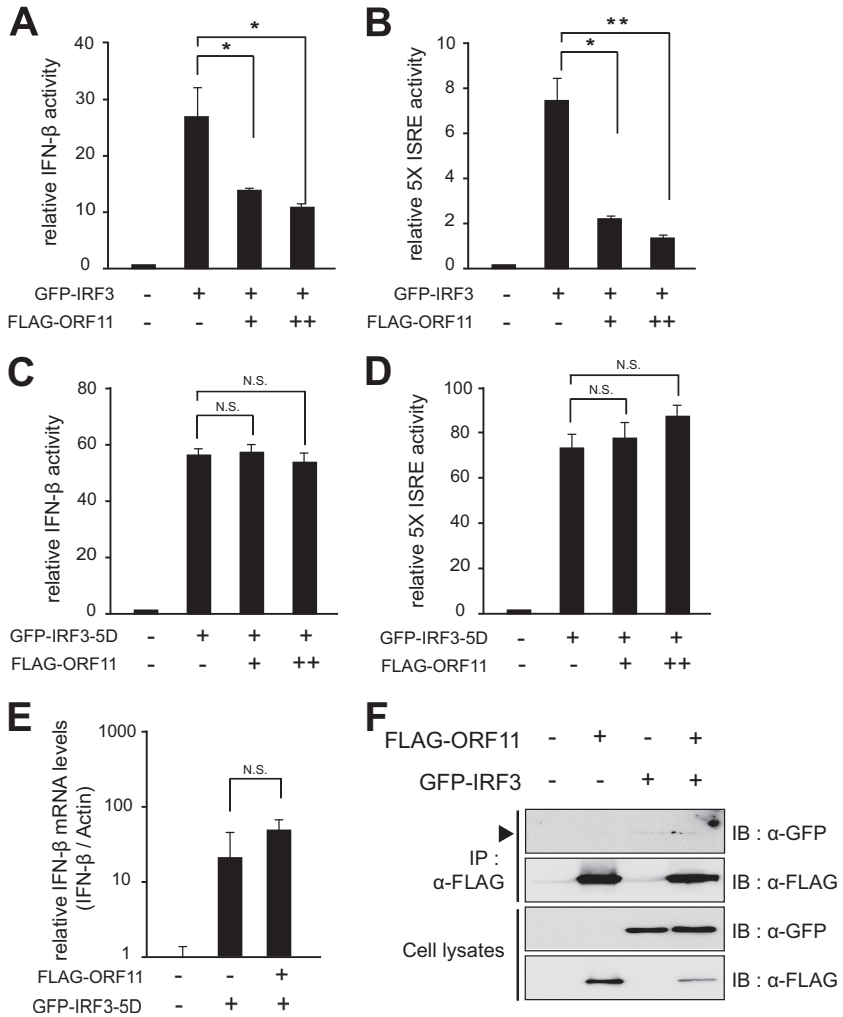

FIG 4 MHV-68 ORF11 inhibits IFN-β promoter activation by IRF3, not by IRF3-5D. (A and B) ORF11 inhibited IRF3-induced IFN-β promoter and 5×ISRE activities. GFP-IRF3 (300 ng) was cotransfected into HEK293T cells with either vector alone or FLAG-ORF11 (250 ng and 500 ng) in the presence of IFN-β-Luc (A) or 5×ISRE-Luc (B). After 24 h, 5×ISRE-Luc and IFN-β-Luc reporter gene activities were measured and normalized by β-gal activities. (C and D) ORF11 did not inhibit transactivation of the IFN-β promoter and 5×ISRE induced by IRF3-5D, a constitutive active mutant of IRF3. GFP-IRF3-5D (300 ng) was cotransfected into HEK293T cells with FLAG-ORF11 (250 ng and 500 ng) in the presence of IFN-β-Luc (C) or 5×ISRE-Luc (D), and the cell lysates were analyzed as described above. (E) ORF11 did not decrease the *Ifnb* mRNA levels induced by IRF3-5D. HEK293T cells were transfected with GFP-IRF3-5D (300 ng) and FLAG-ORF11 (500 ng) for 24 h. Relative *Ifnb* mRNA levels were measured and normalized to actin mRNA levels by RT-qPCR. (F) ORF11 did not directly interact with IRF3. GFP-IRF3 (9 μg) and FLAG-ORF11 (9 μg) were cotransfected into HEK293T cells. After 48 h, the cells were lysed and immunoprecipitated (IP) with α-FLAG. The arrow represents the expected size of GFP-IRF3. The data are shown as means ± standard deviations. *, $P < 0.05$; **, $P < 0.01$ (Student's *t* test).

replication to negatively modulate the host type I interferon response.

ORF11 inhibits IFN-β promoter activated by IRF3, not by IRF3-5D. To further investigate the effect of ORF11 on TBK1-IRF3 activation, the reporter plasmid IFN-β-Luc or 5×ISRE-Luc was cotransfected into HEK293T cells with or without ORF11 in the presence of IRF3. ORF11 efficiently inhibited the activation of IFN-β-Luc and 5×ISRE-Luc by IRF3 (Fig. 4A and B). However, ORF11 had no effect on the promoter activity of IFN-β-Luc and 5×ISRE-Luc activated by IRF3-5D, a constitutively active mutant form of IRF3 (Fig. 4C and D). Consistent with these results, ORF11 transfection failed to decrease the endogenous *Ifnb* mRNA induced by IRF3-5D (Fig. 4E). Our repeated attempts to show physical interaction between ORF11 and IRF3 were not successful, as shown in the coimmunoprecipitation assay (Fig. 4F). These results suggest that ORF11 targets sequence upstream of IRF3 to block IFN production rather than directly targeting IRF3.

ORF11 inhibits the IFN-β promoter activated by TBK1 via direct binding to TBK1. We next examined whether ORF11 targets an upstream kinase of IRF3, TBK1, that is ubiquitously expressed in most cell types. When transfected in HEK293T cells, ORF11 efficiently inhibited the activation of IFN-β-Luc and 5×ISRE-Luc induced by TBK1 in a dose-dependent manner (Fig. 5A and B). Accordingly, ORF11 also decreased the endogenous *Ifnb* mRNA induced by TBK1 in HEK293T cells (Fig. 5C). We further examined direct interaction of ORF11 with TBK1 (Fig. 5D to F). When overexpressed in HEK293T cells, ORF11 was coimmunoprecipitated with TBK1 and colocalized with TBK1 in the cytoplasm of HEK293T cells (Fig. 5D and E). To further confirm the physiological interaction between ORF11 and TBK1, we im-

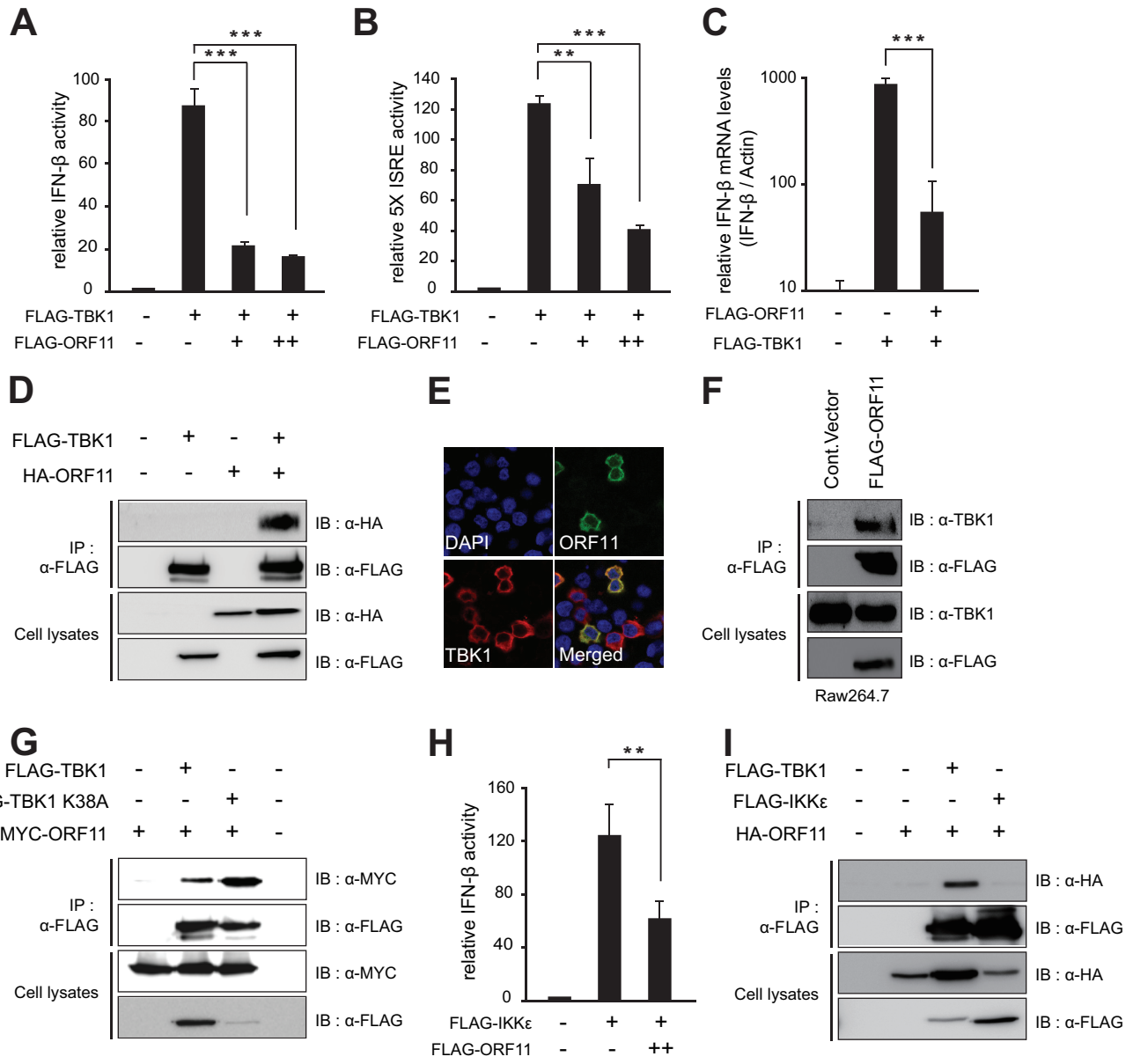

FIG 5 MHV-68 ORF11 inhibits TBK1-induced IFN-β promoter activation via direct binding. (A and B) ORF11 inhibited TBK1-induced IFN-β promoter and 5×ISRE activities. FLAG-TBK1 (100 ng) was cotransfected into HEK293T cells with FLAG-ORF11 (200 ng and 400 ng) in the presence of IFN-β-Luc (A) or 5×ISRE-Luc (B). After 24 h, 5×ISRE-Luc and IFN-β-Luc reporter gene activities were measured and normalized to β-gal activities. (C) ORF11 decreased the *Ifnb* mRNA levels induced by TBK1. HEK293T cells were transfected with FLAG-TBK1 (100 ng) and FLAG-ORF11 (500 ng) for 24 h. Relative *Ifnb* mRNA levels were measured and normalized to the actin mRNA levels by RT-qPCR. (D) Direct interaction of ORF11 with TBK1. FLAG-TBK1 (9 μg) and HA-ORF11 (9 μg) were cotransfected into HEK293T cells. After 48 h, the cells were lysed and immunoprecipitated with α-FLAG. (E) Colocalization of ORF11 and TBK1 in the cytoplasm. HA-ORF11 and FLAG-TBK1 were transfected into HEK293T cells, and the cells were fixed at 24 h. HA-ORF11 and FLAG-TBK1 were stained for ORF11 (FITC; green) and TBK1 (Cy3; red), respectively, while the nuclei were stained with the DNA-intercalating dye DAPI (blue). All of the panels were under a magnification of ×1,000. (F) ORF11 interacted with endogenous TBK1. Raw264.7 cells stably expressing a control vector or FLAG-ORF11 were lysed and immunoprecipitated with α-FLAG and immune blotted with α-TBK1 to detect the endogenous TBK1. (G) ORF11 interacted with a TBK1 kinase null mutant. FLAG-TBK1 K38A (9 μg) or FLAG-TBK1 (9 μg) was cotransfected with MYC-ORF11 (9 μg) into HEK293T cells. After 48 h, the cells were lysed and immunoprecipitated with α-FLAG antibody. (H) ORF11 inhibited IKKε-induced IFN-β promoter activities. FLAG-IKKε (100 ng) was cotransfected into HEK293T cells with FLAG-ORF11 (200 ng, 400 ng) in the presence of IFN-β-Luc. After 28 h, 5×ISRE-Luc and IFN-β-Luc reporter gene activities were measured and normalized as described for panels A and B. (I) ORF11 did not directly interact with IKKε. FLAG-IKKε (9 μg) and HA-ORF11 (9 μg) were cotransfected into HEK293T cells. After 48 h, the cells were lysed and immunoprecipitated with α-FLAG. Each error bar shows means ± standard deviations. **, $P < 0.01$; ***, $P < 0.001$ (Student's *t* test).

munoprecipitated ORF11 in Raw264.7 cells stably expressing FLAG-ORF11 (Fig. 3B, right) and found that ORF11 interacted with endogenous TBK1, suggesting that ORF11 targets TBK1 to inhibit the host type I interferon response during virus infection (Fig. 5F). The interaction of TBK1 with ORF11 was independent of its kinase activity, as shown in strong binding of ORF11 with TBK1 K38A, a kinase null mutant of TBK1 (Fig. 5G). IKKε is another upstream kinase that can activate IRF3 mainly in immune cells. ORF11

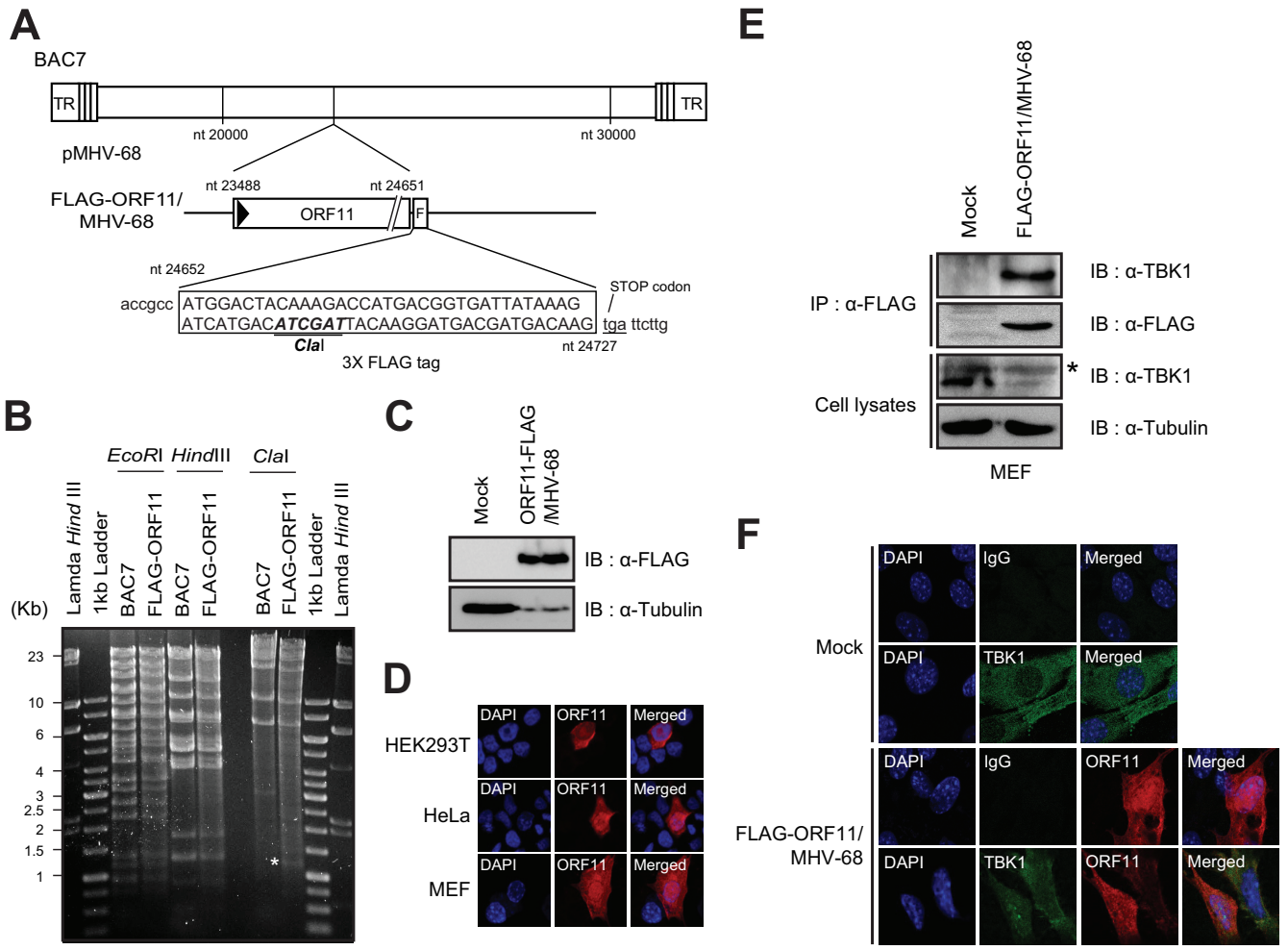

FIG 6 ORF11 interacts with endogenous TBK1 during MHV-68 infection. (A) Schematic diagram of the FLAG-tagged ORF11 recombinant virus (FLAG-ORF11/MHV-68) in the MHV-68 genome. (B) Construction of the FLAG-ORF11/MHV-68 virus. The 3×FLAG sequences were introduced into the ORF11 locus (nt 24652) of the MHV-68 BAC clone (pMHV-68). BAC DNAs for the wild type and FLAG-ORF11 were digested by EcoRI and ClaI and resolved in 0.7% agarose gel. (C) Expression of FLAG-ORF11 during MHV-68 replication. Vero cells were infected with the FLAG-ORF11/MHV-68 virus at an MOI of 0.05 for 72 h cells. The expression of ORF11 was analyzed by Western blotting using anti-FLAG. (D) HEK293T, HeLa, and MEF cells were infected with FLAG-ORF11/MHV-68 at an MOI of 1 for 24 h. (E) Interaction of ORF11 with endogenous TBK1 during virus infection. MEF cells were infected with FLAG-ORF11/MHV-68 (MOI, 1) for 24 h, subjected to immunoprecipitation with α-FLAG, and monitored by immunoblotting with α-TBK1. The asterisk indicates a nonspecific band. (F) Colocalization of ORF11 and TBK1 during viral infection. MEF cells were infected with FLAG-ORF11/MHV-68 at an MOI of 1, and the cells were fixed at 24 h postinfection. ORF11 was stained with Cy3 (red), and TBK1 was stained with FITC (green), while the nuclei were stained with DAPI (blue). All of the panels were under a magnification of ×1,000.

inhibited IKKε-induced IFN-β promoter activation, albeit to a lesser degree than its inhibition of TBK1-activated transactivation (Fig. 5H). There was no direct association of ORF11 and IKKε in transfected HEK293T cells (Fig. 5I). Our results suggest that ORF11 specifically targets TBK1 to inhibit the host type I interferon response.

To further investigate whether ORF11 interacts with TBK1 during virus replication, we constructed a recombinant virus expressing 3×FLAG-tagged ORF11 (FLAG-ORF11/MHV-68) (Fig. 6A). The viral genome integrity of FLAG-ORF11/MHV-68 was confirmed by restriction enzyme mapping (Fig. 6B), and its replication was similar to that of the WT (data not shown). When Vero cells were infected, the FLAG-ORF11/MHV-68 virus expressed the FLAG-ORF11 protein as detected with the anti-FLAG antibody (Fig. 6C). FLAG-ORF11 was expressed in both the cytoplasm and the nucleus of infected HeLa and MEF cells, while it was localized more in the cytoplasm than in the nucleus of infected HEK293T cells (Fig. 6D). Upon infection of FLAG-ORF11/MHV-68 into MEF cells (MOI, 2) for 24 h, FLAG-ORF11 physically interacted with endogenous TBK1 and was colocalized with TBK1, as shown in coimmunoprecipitation and IFA, respectively (Fig. 6E and F). Taken together, these results demonstrate that MHV-68 ORF11 physically interacts with TBK1 in the context of virus replication to inhibit IFN production.

ORF11 blocks IRF3 activation by interfering with the interaction between TBK1 and IRF3. Upon RNA and DNA virus infections, TBK1 plays a critical role in activation of IRF3, such as its phosphorylation, dimerization, and nuclear translocation, leading to transactivation of the IFN-β promoter. We next examined the effect of ORF11-TBK1 interactions on IRF3 activation (Fig. 7). When IRF3 and TBK1 were cotransfected into HEK293T cells with ORF11, ORF11 decreased IRF3 phosphorylation induced by TBK1 in a dose-dependent manner (Fig. 7A). The level of HA-

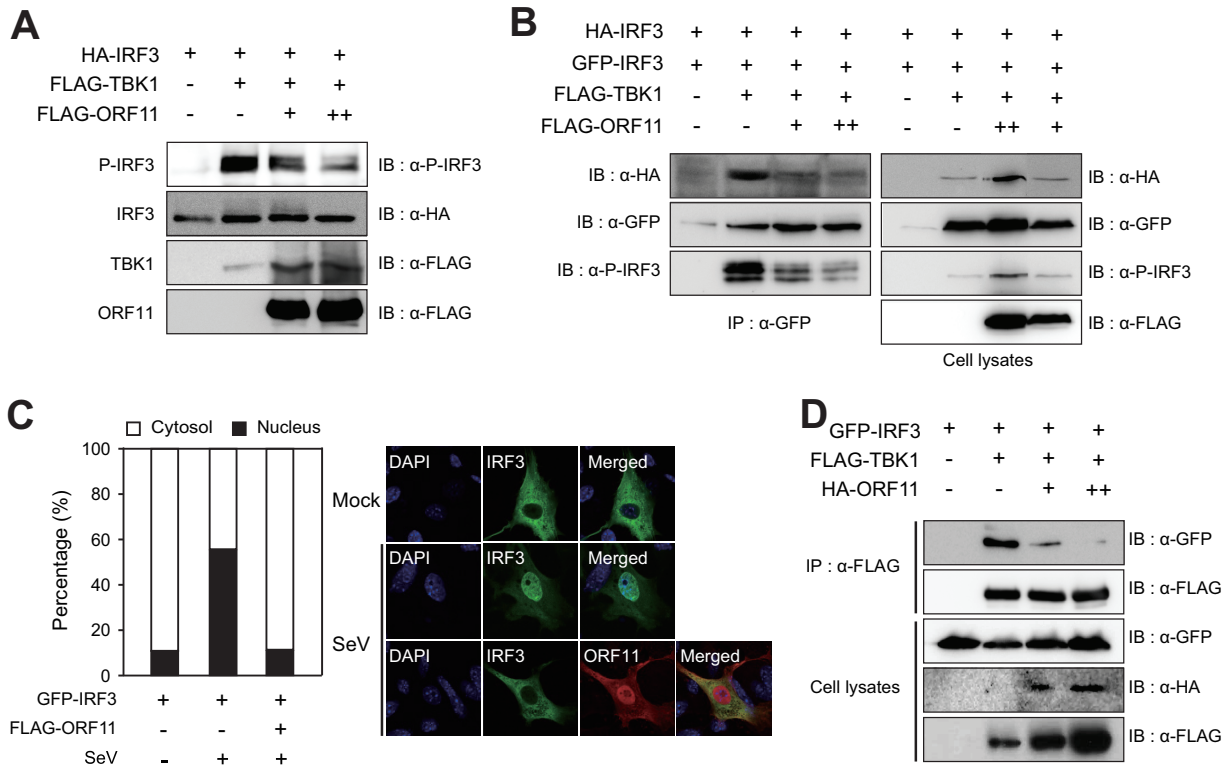

FIG 7 MHV68 ORF11 interferes with TBK1-induced IRF3 activation via abolishing the interactions between TBK1 and IRF3. (A) ORF11 inhibited the phosphorylation of IRF3. HA-IRF3 (300 ng), FLAG-TBK1 (100 ng), and FLAG-ORF11 (500 ng) were cotransfected into HEK293T cells. After 24 h, the transfected cells were harvested and analyzed by Western blotting using α-phospho-IRF3 (Ser396). (B) ORF11 inhibited the dimerization of IRF3. IRF3 with two different tags (HA-IRF3 and GFP-IRF3) (3 μg), FLAG-TBK1 (3 μg), and FLAG-ORF11 (5 μg) were transfected into HEK293T cells. After 24 h, the cells were lysed and immunoprecipitated with α-GFP and analyzed by Western blotting. (C) MEF cells were transfected with GFP-IRF3 (4 μg) and FLAG-ORF11 (6 μg) and were infected with SeV (50 HA units). After 6 h, we examined the location of IRF3 (GFP; green) by immunofluorescence. ORF11 was stained by Cy3 (red), and the nuclei were stained by DAPI (blue). Every sample had more than 100 cells, and the percentage of the cells is shown for cytoplasmic or nuclear localization. All of the panels were under a magnification of ×1,000. (D) ORF11 disrupted the interaction between TBK1 and IRF3. GFP-IRF3 (4 μg), FLAG-TBK1 (5 μg), and HA-ORF11 (4 μg and 9 μg) were cotransfected into HEK293T cells. At 24 h, the cells were lysed and immunoprecipitated with α-FLAG and analyzed by Western blotting.

IRF3 immunoprecipitated with GFP-IRF3 in the presence of TBK1 was decreased with increasing doses of ORF11, indicating that ORF11 inhibited dimer formation of IRF3 induced by TBK1 (Fig. 7B). Furthermore, nuclear translocation of IRF3 following SeV infection (10 HA units) for 6 h was efficiently blocked in MEF cells when ORF11 was overexpressed (Fig. 7C). Since IRF3 is a substrate of TBK1 and ORF11 binds to TBK1, we tested whether ORF11 can interfere with TBK1 and IRF3 interactions. In coimmunoprecipitation assays, the interactions between IRF3 and TBK1 were inhibited by ORF11 (Fig. 7D). These results suggest that ORF11 outcompetes IRF3 for TBK1 binding and subsequently inhibits TBK1-induced IRF3 activation.

The central domain of ORF11 is essential for TBK1 binding and IFN inhibition, while the kinase domain of TBK1 is important for ORF11 binding. The ORF11 protein of MHV-68 consists of 388 amino acids. To map the domain of ORF11 that is required for TBK1 binding and IFN inhibition, we generated ORF11 domain mutants. Since computational structure analysis of the ORF11 protein revealed no currently known domain or motif except weak homology for the 2′-deoxyuridine 5′-triphosphate pyrophosphatase (dUTPase)-like motif (50, 51), we made a series of N terminus and C terminus truncation mutants (Fig. 8A). Coimmunoprecipitation results of ORF11 ΔN1 and ΔC1 mutants with TBK1 showed that both the N terminus (domain I) and C terminus (domain IV) of ORF11 were dispensable for TBK1 binding. However, as shown in the results for ORF11 ΔN2 and ΔC2 mutants, deletion of the central domains (domains II and III) abolished ORF11 and TBK1 interactions. Similarly, ORF11 lost its inhibition of TBK1-mediated IFN-β-Luc transactivation when the central domain of ORF11 was disrupted in ΔN2 and ΔC2 mutants (Fig. 8D), suggesting that the central domain of ORF11 (domains II and III) is required for both TBK1 binding and IFN inhibition of ORF11. To test whether the central domain of ORF11 is sufficient to confer TBK1 binding and IFN inhibition, we constructed ORF11 CD, expressing the central domain (domains II and III) alone, and found that the central domain of ORF11 alone was sufficient for TBK1 binding (Fig. 8B). Furthermore, ORF11 CD was also sufficient to inhibit IRF3 phosphorylation and the IFN-β promoter activity induced by TBK1 (Fig. 8C and D). Taken together, these results suggest that the central domain of ORF11was sufficient to bind and inhibit TBK1, leading to inhibition of IRF3 activation and IFN-β production.

To further map the minimal domain of TBK1 to interact with ORF11, we constructed TBK1 domain mutants, TBK1-KD/ULD and TBK1-KD, according to the previous report (52) (Fig. 9A). TBK1-KD (amino acids [aa]1 to 301) deletes both ULD and SDD/CTD, leaving the kinase domain alone, while TBK1-KD/ULD (aa 1 to 383) contains the kinase domain and ubiquitin-like domain

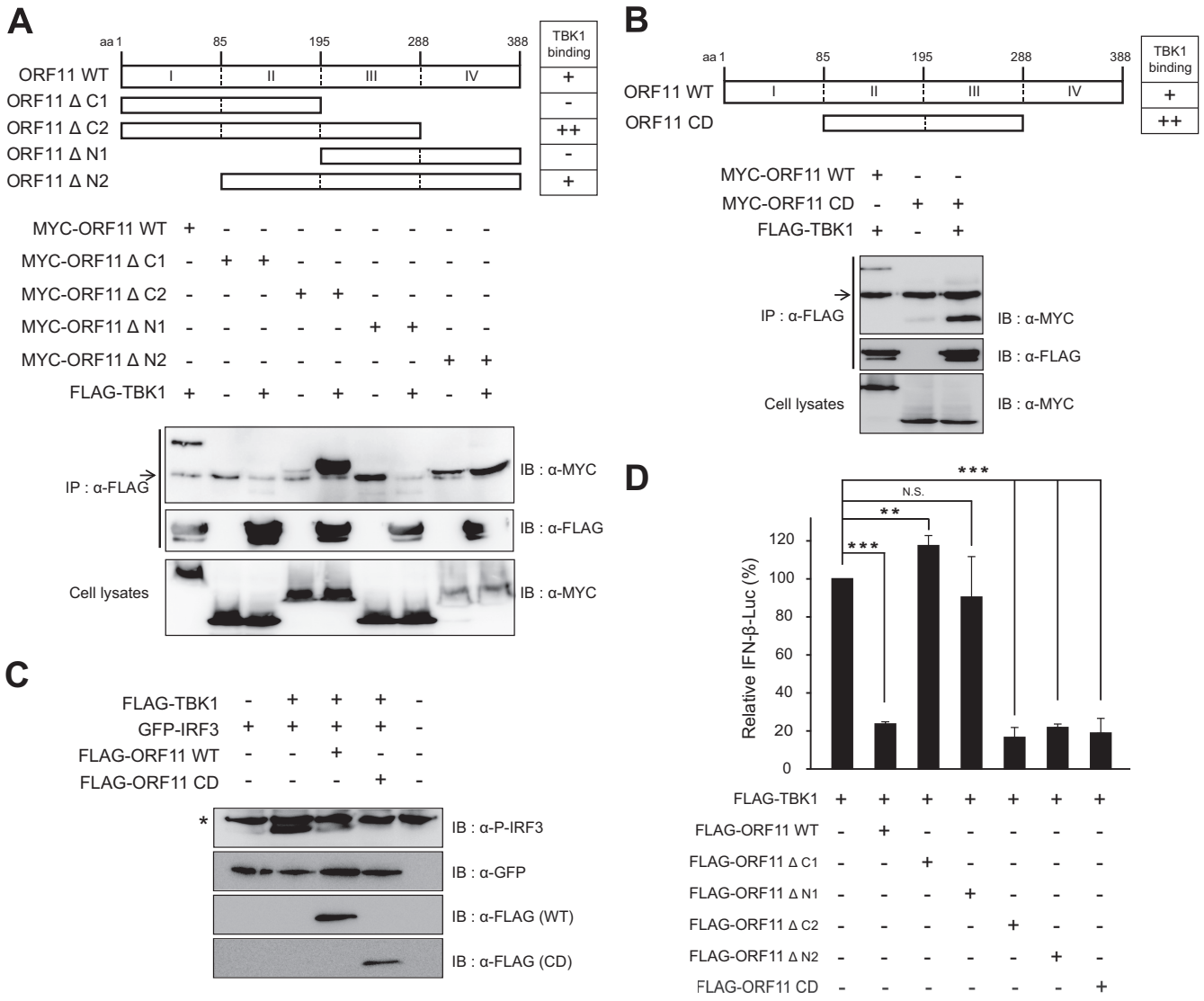

FIG 8 Functional domain mapping of MHV-68 ORF11 required for TBK1 interaction and inhibition. (A) The central domain of ORF11 (CD; aa 85 to 288) was necessary to bind to TBK1. Full-length MYC-ORF11 (WT), ΔC1, ΔC2, ΔN1, or ΔN2 (9 μg) was transfected with FLAG-TBK1 (9 μg) into HEK293T cells. After 48 h, the cells were lysed and immunoprecipitated with α-FLAG and analyzed by Western blotting. An arrow indicates IgG bands. (B) The central domain of ORF11 (CD; aa 85 to 288) was sufficient for TBK1 binding. Full-length MYC-ORF11 (WT) (9 μg) and the ORF11 CD (9 μg) were transfected with FLAG-TBK1 (9 μg) into HEK293T cells. After 48 h, the cells were lysed and immunoprecipitated with α-FLAG and analyzed by Western blotting. An arrow indicates IgG bands, while the asterisk indicates a nonspecific band, serving as a loading control. (C) ORF11 CD was sufficient to inhibit the phosphorylation of IRF3 by TBK1. FLAG-TBK1 (100 ng) and GFP-IRF3 (300 ng) were cotransfected with WT FLAG-ORF11 or FLAG-ORF11 CD (500 ng) into HEK293T cells. After 24 h, the transfected cells were harvested and analyzed by Western blotting using α-phosphoIRF3 (Ser396). N.S. indicates nonspecific bands. (D) ORF11 CD was sufficient to inhibit TBK1-induced IFN-β promoter activity. Full-length FLAG-ORF11 (WT), ΔC1, ΔC2, ΔN1, ΔN2, or CD (400 ng) was transfected with FLAG TBK1 (100 ng) into HEK293T cells. IFN-β-Luc reporter gene activities were measured and normalized to β-gal activities. Each error bar shows means ± standard deviations. **, $P < 0.01$; ***, $P < 0.001$ (Student's t test).

and lacks two coiled-coil domains at the C terminus, which serve as a scaffold/dimerization domain (SDD) (52–54). Consistent with the previous report (52), these two mutants failed to activate IFN-β production in reporter assays (Fig. 9A). In our coimmunoprecipitation assays, TBK1-KD bound to ORF11 at a level similar to that of full-length TBK1, while TBK1-KD/ULD showed no or little binding to TBK1 (Fig. 9B), suggesting that the TBK1 kinase domain is a minimal domain required for ORF11 interaction.

DISCUSSION

While the production of type I interferon is a fundamental host response to combat viral invasion, viral pathogens develop multiple strategies to subvert such host IFN responses. Here, we confirmed that lytic MHV-68 infection blocks type I interferon signaling and identified MHV-68 ORF11 as a negative regulator of interferon-β production via an unbiased genomic approach using a transposon mutant library of MHV-68. ORF11 expression inhibited activation of the IFN-β promoter by various factors. ORF11 interacted directly with both overexpressed and endogenous TBK1, which was further confirmed in the context of virus replication using a recombinant virus expressing FLAG-ORF11. Interactions between ORF11 and TBK1 disrupted the interaction between TBK1 and IRF3, thereby blocking IRF3 phosphorylation,

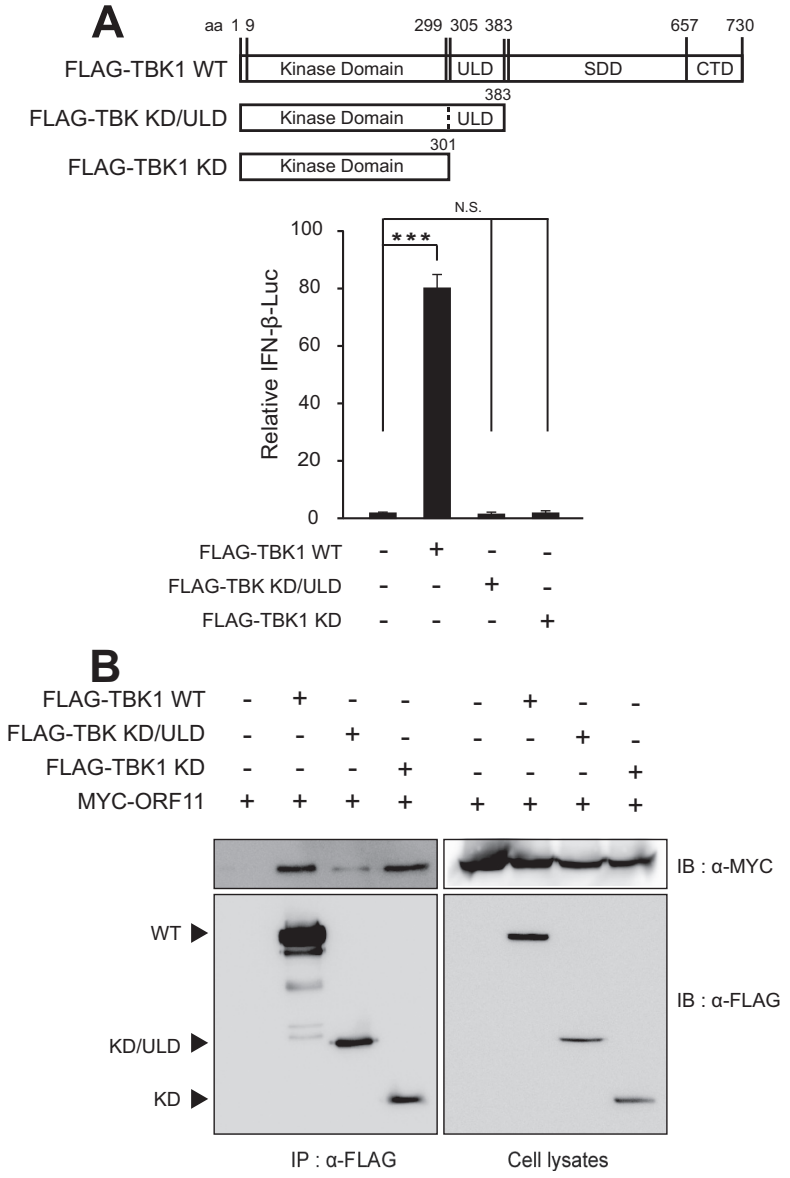

FIG 9 Kinase domain of TBK1 is sufficient to bind to MHV-68 ORF11. (A) Activity of TBK1 domain mutant constructs. The upper panel illustrates schematic diagrams of WT TBK1 and mutants containing the kinase domain (KD), ubiquitin-like domain (ULD), scaffold/dimerization domain (SDD), and/or C-terminal domain (CTD). FLAG-TBK1 WT, KD/ULD, or KD (100 ng) was cotransfected with full-length ORF11 into HEK293T cells. IFN-β-Luc promoter activities were measured and normalized by β-gal activities. (B) Kinase domain of TBK1 is sufficient to bind to ORF11. FLAG-TBK1 WT, KD/ULD, or KD (9 μg) was cotransfected with MYC-ORF11 (9 μg) into HEK293T cells. After 48 h, the cells were lysed, immune precipitated with α-FLAG, and analyzed by Western blotting. Each error bar shows means ± standard deviations. ***, $P < 0.001$ (Student's *t* test).

dimerization, and nuclear translocation. The central domain of ORF11 was necessary and sufficient for both TBK1 binding and IFN-β promoter inhibition, while the kinase domain of TBK1 was the minimal domain required for interaction with ORF11. To our knowledge, MHV-68 ORF11 is the first viral factor that is identified to block TBK1 function among the genes of gammaherpesviruses.

TBK1 functions as a key node protein in several cell signaling pathways, including antiviral innate immune response, autophagy related to bacterial invasion, cell growth, and proliferation (55). Among them, antiviral innate immune activity of TBK1 has been the most extensively studied. TBK1 activities are tightly regulated in various ways, such as phosphorylation, ubiquitination, kinase activity modulation, and prevention of functional TBK1-containing complexes (55, 56). Several viral factors have been reported to modulate the TBK1 activity to circumvent IFN responses (56). The $\gamma_1$34.5 protein of herpes simplex virus type 1 (HSV-1) and the NS3 protein of hepatitis C virus (HCV) were shown to directly interact with TBK1, which disrupts the interaction of TBK1 and IRF3 (57–59). ORF11 has a mechanism similar to those of HSV $\gamma_1$34.5 and HCV NS3 proteins in that it directly binds to TBK1 and blocks IRF3 activation by inhibiting the interactions of TBK1 and IRF3, but there is no sequence homology among these proteins (data not shown). However, the fact that

viruses encode viral proteins targeting TBK1-mediated signaling pathways highlights a critical role of TBK1 in antiviral immunity. Although TBK1 and IKKε have similar biochemical properties *in vitro*, they have very distinct functions *in vivo* (60, 61). TBK1 is activated by pattern recognition receptors, such as Toll-like receptors, and intracellular receptors, such as RIG-I, MDA5, and DAI, and it phosphorylates IRF3 and IRF7 and other target proteins (62). TBK1 is essential for the activation of type I IFN *in vivo*, while IKKε is not. In fact, IKKε is required for the activation of IFN-stimulated genes *in vivo* but is not required for IFN expression. IKKε functions by phosphorylating a specific serine residue in the transcription factor STAT1, thereby controlling the assembly of IFN-inducible transcription factor complexes (60, 61). Although TBK1 is highly homologous to IKKε, TBK1, not IKKε, was required for controlling DNA virus infection (25, 26). It is interesting that ORF11 bound to TBK1, not to IKKε, a closely related kinase, although it inhibited the IFN-β promoter activity induced by both TBK1 and IKKε, suggesting that ORF11 indirectly inhibits the IKKε signaling or targets the sequence downstream of IKKε in a TBK1-independent manner. Although HSV $\gamma_1$34.5 and HCV NS3 proteins inhibited the IKKε signaling, interaction of HSV $\gamma_1$34.5 or HCV NS3 proteins with IKKε has not been shown.

The ORF11 protein of MHV-68 consists of 388 amino acids and is conserved among gammaherpesviruses. The maximum identities of homologues between MHV-68 and KSHV or MHV-68 and EBV are 22% or 24%, respectively, while those between KSHV ORF11 and EBV LF2 are up to 43%. All of these ORF11 homologues are predicted to contain a limited motif related to herpesviral dUTPase (50), but their actual dUTPase activities have never been shown. While little has been studied about the function of KSHV ORF11, multiple functions of EBV LF2 were reported (63). Interestingly, EBV LF2 was also shown to inhibit type I IFN production (63). EBV LF2 was identified from a screening of EBV ORFs for its ability to block SeV-induced IFN-α promoter activity. EBV LF2 directly binds to IRF7 and blocks IRF7 dimerization rather than affecting phosphorylation and nuclear translocation of IRF7. However, the mechanism of EBV LF2 seems to differ from that of MHV-68 ORF11 in that EBV LF2 had no effect on IRF3-induced ISRE activation (63). Therefore, MHV-68 ORF11 and EBV LF2 may have a similar function via independent mechanisms during virus replication. Recently, a conserved viral dUTPase (ORF54) of MHV-68 was shown to downregulate type I IFN signaling by inducing the degradation of the type I interferon receptor protein independent of its dUTPase enzymatic activity (64). KSHV ORF10, with weak homology to viral dUTPase, was also shown to block IFN-mediated signal transduction by forming inhibitory complexes with the type I IFN receptor subunit (65). Moreover, the KSHV viral dUTPase ORF54 was reported to downregulate a ligand for the NK-activating receptor NKp44 without requiring viral dUTPase (66). Although it is not clear whether viral dUTPase motifs of MHV-68 ORF11 would contribute to its inhibition of type I IFN production, it is interesting that all ORFs of gammaherpesviruses with predicted homology to viral dUTPase confer the functions to inhibit host innate immunity, especially the type I IFN system, via various mechanisms.

It has been shown that type I IFNs have roles not only in controlling acute replication of MHV-68 but also in modulating latent gene expression and inhibiting viral reactivation during latency (67). Given that MHV-68 ORF11 is a virion-associated tegument protein (48), the role of ORF11 in inhibiting type I IFNs is 2-fold: it can modulate virus replication in permissive fibroblasts and the host immune milieu in immune cells, such as macrophages or dendritic cells. Our results indicate that ORF11 efficiently blocked type I IFN production from both fibroblasts and macrophages, supporting this notion (Fig. 2 and 3). Since macrophages or dendritic cells are *in vivo* latent reservoirs of MHV-68 in addition to B cells, ORF11 may affect latent infection in addition to acute lytic replication, possibly by regulating reactivation frequency. Consistent with these results, ORF11 deficiency led to significantly reduced acute replication in the lung and a delay in seeding to the spleen for latency following intranasal infection (38, 48). However, we and others found little difference between ORF11-deficient viruses and their revertants in viral growth in cultured cells (Fig. 2), suggesting that the type I IFN response is more critical in controlling virus replication *in vivo* than *in vitro*.

Our screening results suggest that multiple viral proteins act together to curtail the host type I IFN response during gammaherpesvirus infection (Fig. 1). Although each viral factor was necessary, it did not appear to be sufficient for blocking the IFN pathway. Since viral proteins are expressed over the course of infection with different kinetics, these factors may be required for the virus to efficiently replicate in an optimal host immune milieu. Nevertheless, it is unclear why our identified hits, such as ORF36 and ORF11, mainly downregulated IFN-β production despite the fact that our initial screening was designed to identify a negative regulator of the type I IFN signaling pathway that would inhibit the 5×ISRE-Luc activity following IFN-β treatment. However, it is plausible to reason that exogenously added IFN-β induces stronger type I IFN production via positive feedback, leading to further activation of 5×ISRE-Luc in our screenings. Thus, the ORF11 mutant may fail to block the second wave of type I IFN production. These results suggest that blocking the upstream sequence of IFN-β production would be more effective than targeting its downstream sequence to evade host immune responses.

Taken together, identification of ORF11 from a cell-based screening using the single-gene mutant virus library accentuates the critical role of ORF11 in blocking type I IFN production in the context of virus replication and highlights the central function of TBK1 in DNA virus infection. Taken together, the virion-associated ORF11 may function as a novel viral immune modulator that regulates the virus life cycle by inhibiting type I interferon production via targeting TBK1 and serves as an important candidate for vaccine development.

ACKNOWLEDGMENTS

We thank Ren Sun, Seungmin Hwang, Gehong Cheng, Andrew Bowie, Kate Fitzgerald, Joo-Young Lee, and Suk-Jo Kang for their plasmids and contributions.

This work was supported by National Research Foundation grants funded by the Korean Government (2009-0080895 and 2012R1A1A2004532) and a grant from the National R&D Program for Cancer Control, Ministry of Health, Welfare and Family Affairs, Republic of Korea (0920170).

REFERENCES

1. **Chin YE, Kitagawa M, Kuida K, Flavell RA, Fu XY.** 1997. Activation of the STAT signaling pathway can cause expression of caspase 1 and apoptosis. Mol. Cell. Biol. **17**:5328–5337.
2. **Gale M, Katze MG.** 1998. Molecular mechanisms of interferon resistance mediated by viral-directed inhibition of PKR, the interferon-induced protein kinase. Pharmacol. Ther. **78**:29–46. http://dx.doi.org/10.1016/S0163-7258(97)00165-4.

3. **Pellegrini S, John J, Shearer M, Kerr IM, Stark GR.** 1989. Use of a selectable marker regulated by alpha interferon to obtain mutations in the signaling pathway. Mol. Cell. Biol. **9:**4605–4612.
4. **Symons JA, Alcami A, Smith GL.** 1995. Vaccinia virus encodes a soluble type-I interferon receptor of novel structure and broad species-specificity. Cell **81:**551–560. http://dx.doi.org/10.1016/0092-8674(95)90076-4.
5. **Hwang SY, Hertzog PJ, Holland KA, Sumarsono SH, Tymms MJ, Hamilton JA, Whitty G, Bertoncello I, Kola I.** 1995. A null mutation in the gene encoding a type I interferon receptor component eliminates antiproliferative and antiviral responses to interferons alpha and beta and alters macrophage responses. Proc. Natl. Acad. Sci. U. S. A. **92:**11284–11288. http://dx.doi.org/10.1073/pnas.92.24.11284.
6. **Deonarain R, Alcami A, Alexiou M, Dallman MJ, Gewert DR, Porter AC.** 2000. Impaired antiviral response and alpha/beta interferon induction in mice lacking beta interferon. J. Virol. **74:**3404–3409. http://dx.doi.org/10.1128/JVI.74.7.3404-3409.2000.
7. **Gibbert K, Joedicke JJ, Meryk A, Trilling M, Francois S, Duppach J, Kraft A, Lang KS, Dittmer U.** 2012. Interferon-alpha subtype 11 activates NK cells and enables control of retroviral infection. PLoS Pathog. **8:**e1002868. http://dx.doi.org/10.1371/journal.ppat.1002868.
8. **van den Broek MF, Muller U, Huang S, Aguet M, Zinkernagel RM.** 1995. Antiviral defense in mice lacking both alpha/beta and gamma interferon receptors. J. Virol. **69:**4792–4796.
9. **Malmgaard L.** 2004. Induction and regulation of IFNs during viral infections. J. Interferon Cytokine Res. **24:**439–454. http://dx.doi.org/10.1089/1079990041689665.
10. **Hiscott J.** 2007. Triggering the innate antiviral response through IRF-3 activation. J. Biol. Chem. **282:**15325–15329. http://dx.doi.org/10.1074/jbc.R700002200.
11. **Fitzgerald KA, McWhirter SM, Faia KL, Rowe DC, Latz E, Golenbock DT, Coyle AJ, Liao SM, Maniatis T.** 2003. IKKepsilon and TBK1 are essential components of the IRF3 signaling pathway. Nat. Immunol. **4:**491–496. http://dx.doi.org/10.1038/ni921.
12. **Sharma S, ten Oever BR, Grandvaux N, Zhou GP, Lin R, Hiscott J.** 2003. Triggering the interferon antiviral response through an IKK-related pathway. Science **300:**1148–1151. http://dx.doi.org/10.1126/science.1081315.
13. **Hemmi H, Takeuchi O, Sato S, Yamamoto M, Kaisho T, Sanjo H, Kawai T, Hoshino K, Takeda K, Akira S.** 2004. The roles of two IkappaB kinase-related kinases in lipopolysaccharide and double stranded RNA signaling and viral infection. J. Exp. Med. **199:**1641–1650. http://dx.doi.org/10.1084/jem.20040520.
14. **McWhirter SM, Fitzgerald KA, Rosains J, Rowe DC, Golenbock DT, Maniatis T.** 2004. IFN-regulatory factor 3-dependent gene expression is defective in Tbk1-deficient mouse embryonic fibroblasts. Proc. Natl. Acad. Sci. U. S. A. **101:**233–238. http://dx.doi.org/10.1073/pnas.2237236100.
15. **Hacker H, Redecke V, Blagoev B, Kratchmarova I, Hsu LC, Wang GG, Kamps MP, Raz E, Wagner H, Hacker G, Mann M, Karin M.** 2006. Specificity in Toll-like receptor signalling through distinct effector functions of TRAF3 and TRAF6. Nature **439:**204–207. http://dx.doi.org/10.1038/nature04369.
16. **Ishii KJ, Kawagoe T, Koyama S, Matsui K, Kumar H, Kawai T, Uematsu S, Takeuchi O, Takeshita F, Coban C, Akira S.** 2008. TANK-binding kinase-1 delineates innate and adaptive immune responses to DNA vaccines. Nature **451:**725–729. http://dx.doi.org/10.1038/nature06537.
17. **Oganesyan G, Saha SK, Guo B, He JQ, Shahangian A, Zarnegar B, Perry A, Cheng G.** 2006. Critical role of TRAF3 in the Toll-like receptor-dependent and -independent antiviral response. Nature **439:**208–211. http://dx.doi.org/10.1038/nature04374.
18. **Ryzhakov G, Randow F.** 2007. SINTBAD, a novel component of innate antiviral immunity, shares a TBK1-binding domain with NAP1 and TANK. EMBO J. **26:**3180–3190. http://dx.doi.org/10.1038/sj.emboj.7601743.
19. **Sasai M, Shingai M, Funami K, Yoneyama M, Fujita T, Matsumoto M, Seya T.** 2006. NAK-associated protein 1 participates in both the TLR3 and the cytoplasmic pathways in type I IFN induction. J. Immunol. **177:**8676–8683. http://www.jimmunol.org/content/177/12/8676.
20. **Stetson DB, Medzhitov R.** 2006. Recognition of cytosolic DNA activates an IRF3-dependent innate immune response. Immunity **24:**93–103. http://dx.doi.org/10.1016/j.immuni.2005.12.003.
21. **Chau TL, Gioia R, Gatot JS, Patrascu F, Carpentier I, Chapelle JP, O'Neill L, Beyaert R, Piette J, Chariot A.** 2008. Are the IKKs and IKK-related kinases TBK1 and IKK-epsilon similarly activated? Trends Biochem. Sci. **33:**171–180. http://dx.doi.org/10.1016/j.tibs.2008.01.002.
22. **Guo B, Cheng G.** 2007. Modulation of the interferon antiviral response by the TBK1/IKKi adaptor protein TANK. J. Biol. Chem. **282:**11817–11826. http://dx.doi.org/10.1074/jbc.M700017200.
23. **Chen H, Sun H, You F, Sun W, Zhou X, Chen L, Yang J, Wang Y, Tang H, Guan Y, Xia W, Gu J, Ishikawa H, Gutman D, Barber G, Qin Z, Jiang Z.** 2011. Activation of STAT6 by STING is critical for antiviral innate immunity. Cell **147:**436–446. http://dx.doi.org/10.1016/j.cell.2011.09.022.
24. **Ishikawa H, Barber GN.** 2008. STING is an endoplasmic reticulum adaptor that facilitates innate immune signalling. Nature **455:**674–678. http://dx.doi.org/10.1038/nature07317.
25. **Perry A, Chow E, Goodnough J, Yeh W-C, Cheng G.** 2004. Differential requirement for TANK-binding kinase-1 in type I interferon responses to toll-like receptor activation and viral infection. J. Exp. Med. **199:**1651–1658. http://dx.doi.org/10.1084/jem.20040528.
26. **Miyahira A, Shahangian A, Hwang S, Sun R, Cheng G.** 2009. TANK-binding kinase-1 plays an important role during in vitro and in vivo type I IFN responses to DNA virus infections. J. Immunol. **182:**2248–2257. http://dx.doi.org/10.4049/jimmunol.0802466.
27. **Moore PS, Chang Y.** 2001. Kaposi's sarcoma-associated herpesvirus, p 2803–2833. *In* Knipe DM, Howley PM, Griffin DE, Lamb RA, Martin MA, Roizman B, Straus SE (ed), Fields virology, 4th ed, vol 2. Lippincott Williams and Wilkins, Philadelphia, PA.
28. **Rickinson AB, Kieff E.** 2001. Epstein-Barr virus, p 2575–2628. *In* Knipe DM, Howley PM, Griffin DE, Lamb RA, Martin MA, Roizman B, Straus SE (ed), Fields virology, 4th ed, vol 2. Lippincott Williams and Wilkins, Philadelphia, PA.
29. **Doherty PC, Christensen JP, Belz GT, Stevenson PG, Sangster MY.** 2001. Dissecting the host response to a gamma-herpesvirus. Philos. Trans. R. Soc. London Ser. B Biol. Sci. **356:**581–593. http://dx.doi.org/10.1098/rstb.2000.0786.
30. **Nash AA, Dutia BM, Stewart JP, Davison AJ.** 2001. Natural history of murine gamma-herpesvirus infection. Philos. Trans. R. Soc. London Ser. B Biol. **356:**569–579. http://dx.doi.org/10.1098/rstb.2000.0779.
31. **Speck SH, Virgin HW.** 1999. Host and viral genetics of chronic infection: a mouse model of gamma-herpesvirus pathogenesis. Curr. Opin. Microbiol. **2:**403–409. http://dx.doi.org/10.1016/S1369-5274(99)80071-X.
32. **Virgin HW, Speck SH.** 1999. Unraveling immunity to gamma-herpesviruses: a new model for understanding the role of immunity in chronic virus infection. Curr. Opin. Immunol. **11:**371–379. http://dx.doi.org/10.1016/S0952-7915(99)80063-6.
33. **Flaño E, Kim I-J, Woodland D, Blackman M.** 2002. Gamma-herpesvirus latency is preferentially maintained in splenic germinal center and memory B cells. J. Exp. Med. **196:**1363–1372. http://dx.doi.org/10.1084/jem.20020890.
34. **Stewart JP, Usherwood EJ, Ross A, Dyson H, Nash T.** 1998. Lung epithelial cells are a major site of murine gammaherpesvirus persistence. J. Exp. Med. **187:**1941–1951. http://dx.doi.org/10.1084/jem.187.12.1941.
35. **Sunil-Chandra NP, Efstathiou S, Arno J, Nash AA.** 1992. Virological and pathological features of mice infected with murine gamma-herpesvirus 68. J. Gen. Virol. **73**(Part 9):2347–2356. http://dx.doi.org/10.1099/0022-1317-73-9-2347.
36. **Weck KE, Kim SS, Virgin HW, Speck SH.** 1999. B cells regulate murine gammaherpesvirus 68 latency. J. Virol. **73:**4651–4661.
37. **Weck KE, Kim SS, Virgin HW, Speck SH.** 1999. Macrophages are the major reservoir of latent murine gammaherpesvirus 68 in peritoneal cells. J. Virol. **73:**3273–3283.
38. **Song MJ, Hwang SM, Wong WH, Wu TT, Lee SM, Liao HI, Sun R.** 2005. Identification of viral genes essential for replication of murine gamma-herpesvirus 68 using signature-tagged mutagenesis. Proc. Natl. Acad. Sci. U. S. A. **102:**3805–3810. http://dx.doi.org/10.1073/pnas.0404521102.
39. **Paludan SR, Bowie AG, Horan KA, Fitzgerald KA.** 2011. Recognition of herpesviruses by the innate immune system. Nat. Rev. Immunol. **11:**143–154. http://dx.doi.org/10.1038/nri2937.
40. **Hwang S, Maloney NS, Bruinsma MW, Goel G, Duan E, Zhang L, Shrestha B, Diamond MS, Dani A, Sosnovtsev SV, Green KY, Lopez-Otin C, Xavier RJ, Thackray LB, Virgin HW.** 2012. Nondegradative role of Atg5-Atg12/ Atg16L1 autophagy protein complex in antiviral activity of interferon gamma. Cell Host Microbe **11:**397–409. http://dx.doi.org/10.1016/j.chom.2012.03.002.
41. **Smith GA, Enquist LW.** 1999. Construction and transposon mutagenesis in Escherichia coli of a full-length infectious clone of pseudorabies virus, an alphaherpesvirus. J. Virol. **73:**6405–6414.
42. **Wu TT, Usherwood EJ, Stewart JP, Nash AA, Sun R.** 2000. Rta of murine gammaherpesvirus 68 reactivates the complete lytic cycle from

latency. J. Virol. **74:**3659–3667. http://dx.doi.org/10.1128/JVI.74.8.3659-3667.2000.
43. **Tischer BK, von Einem J, Kaufer B, Osterrieder N.** 2006. Two-step Red-mediated recombination for versatile high-efficiency markerless DNA manipulation in Escherichia coli. Biotechniques **40:**191–197. http://dx.doi.org/10.2144/000112096.
44. **Hwang SM, Kim KS, Flano E, Wu TT, Tong LM, Park AN, Song MJ, Sanchez DJ, O'Connell RM, Cheng GH, Sun R.** 2009. Conserved herpesviral kinase promotes viral persistence by inhibiting the IRF-3-mediated type I interferon response. Cell Host. Microbe **5:**166–178. http://dx.doi.org/10.1016/j.chom.2008.12.013.
45. **Ahn JW, Powell KL, Kellam P, Alber DG.** 2002. Gammaherpesvirus lytic gene expression as characterized by DNA array. J. Virol. **76:**6244–6256. http://dx.doi.org/10.1128/JVI.76.12.6244-6256.2002.
46. **Ebrahimi B, Dutia BM, Roberts KL, Garcia-Ramirez JJ, Dickinson P, Stewart JP, Ghazal P, Roy DJ, Nash AA.** 2003. Transcriptome profile of murine gammaherpesvirus-68 lytic infection. J. Gen. Virol. **84:**99–109. http://dx.doi.org/10.1099/vir.0.18639-0.
47. **Martinez-Guzman D, Rickabaugh T, Wu TT, Brown H, Cole S, Song MJ, Tong LM, Sun R.** 2003. Transcription program of murine gammaherpesvirus 68. J. Virol. **77:**10488–10503. http://dx.doi.org/10.1128/JVI.77.19.10488-10503.2003.
48. **Boname JM, May JS, Stevenson PG.** 2005. Murine gammaherpesvirus 68 open reading frame 11 encodes a nonessential virion component. J. Virol. **79:**3163–3168. http://dx.doi.org/10.1128/JVI.79.5.3163-3168.2005.
49. **Kato H, Takeuchi O, Sato S, Yoneyama M, Yamamoto M, Matsui K, Uematsu S, Jung A, Kawai T, Ishii KJ, Yamaguchi O, Otsu K, Tsujimura T, Koh CS, Sousa CRE, Matsuura Y, Fujita T, Akira S.** 2006. Differential roles of MDA5 and RIG-I helicases in the recognition of RNA viruses. Nature **441:**101–105. http://dx.doi.org/10.1038/nature04734.
50. **Davison AJ, Stow ND.** 2005. New genes from old: redeployment of dUTPase by herpesviruses. J. Virol. **79:**12880–12892. http://dx.doi.org/10.1128/JVI.79.20.12880-12892.2005.
51. **Persson R, McGeehan J, Wilson KS.** 2005. Cloning, expression, purification, and characterisation of the dUTPase encoded by the integrated Bacillus subtilis temperate bacteriophage SPbeta. Protein Expr. Purif. **42:**92–99. http://dx.doi.org/10.1016/j.pep.2005.02.013.
52. **Ikeda F, Hecker CM, Rozenknop A, Nordmeier RD, Rogov V, Hofmann K, Akira S, Dotsch V, Dikic I.** 2007. Involvement of the ubiquitin-like domain of TBK1/IKK-i kinases in regulation of IFN-inducible genes. EMBO J. **26:**3451–3462. http://dx.doi.org/10.1038/sj.emboj.7601773.
53. **Tu D, Zhu Z, Zhou AY, Yun CH, Lee KE, Toms AV, Li Y, Dunn GP, Chan E, Thai T, Yang S, Ficarro SB, Marto JA, Jeon H, Hahn WC, Barbie DA, Eck MJ.** 2013. Structure and ubiquitination-dependent activation of TANK-binding kinase 1. Cell Rep. **3:**747–758. http://dx.doi.org/10.1016/j.celrep.2013.01.033.
54. **Larabi A, Devos JM, Ng SL, Nanao MH, Round A, Maniatis T, Panne D.** 2013. Crystal structure and mechanism of activation of TANK-binding kinase 1. Cell Rep. **3:**734–746. http://dx.doi.org/10.1016/j.celrep.2013.01.034.
55. **Helgason E, Phung QT, Dueber EC.** 2013. Recent insights into the complexity of Tank-binding kinase 1 signaling networks: the emerging role of cellular localization in the activation and substrate specificity of TBK1. FEBS Lett. **587:**1230–1237. http://dx.doi.org/10.1016/j.febslet.2013.01.059.
56. **Zhao W.** 2013. Negative regulation of TBK1-mediated antiviral immunity. FEBS Lett. **587:**542–548. http://dx.doi.org/10.1016/j.febslet.2013.01.052.
57. **Otsuka M, Kato N, Moriyama M, Taniguchi H, Wang Y, Dharel N, Kawabe T, Omata M.** 2005. Interaction between the HCV NS3 protein and the host TBK1 protein leads to inhibition of cellular antiviral responses. Hepatology **41:**1004–1012. http://dx.doi.org/10.1002/hep.20666.
58. **Verpooten D, Feng Z, Valyi-Nagy T, Ma Y, Jin H, Yan Z, Zhang C, Cao Y, He B.** 2009. Dephosphorylation of eIF2alpha mediated by the gamma134.5 protein of herpes simplex virus 1 facilitates viral neuroinvasion. J. Virol. **83:**12626–12630. http://dx.doi.org/10.1128/JVI.01431-09.
59. **Ma Y, Jin H, Valyi-Nagy T, Cao Y, Yan Z, He B.** 2012. Inhibition of TANK binding kinase 1 by herpes simplex virus 1 facilitates productive infection. J. Virol. **86:**2188–2196. http://dx.doi.org/10.1128/JVI.05376-11.
60. **Tenoever BR, Ng SL, Chua MA, McWhirter SM, Garcia-Sastre A, Maniatis T.** 2007. Multiple functions of the IKK-related kinase IKKepsilon in interferon-mediated antiviral immunity. Science **315:**1274–1278. http://dx.doi.org/10.1126/science.1136567.
61. **Ng MH, Ho TH, Kok KH, Siu KL, Li J, Jin DY.** 2011. MIP-T3 is a negative regulator of innate type I IFN response. J. Immunol. **187:**6473–6482. http://dx.doi.org/10.4049/jimmunol.1100719.
62. **Clement JF, Meloche S, Servant MJ.** 2008. The IKK-related kinases: from innate immunity to oncogenesis. Cell Res. **18:**889–899. http://dx.doi.org/10.1038/cr.2008.273.
63. **Wu L, Fossum E, Joo CH, Inn KS, Shin YC, Johannsen E, Hutt-Fletcher LM, Hass J, Jung JU.** 2009. Epstein-Barr virus LF2: an antagonist to type I interferon. J. Virol. **83:**1140–1146. http://dx.doi.org/10.1128/JVI.00602-08.
64. **Leang RS, Wu TT, Hwang SM, Liang LT, Tong LM, Truong JT, Sun R.** 2011. The anti-interferon activity of conserved viral dUTPase ORF54 is essential for an effective MHV-68 infection. PLoS Pathog. **7:**e1002292. http://dx.doi.org/10.1371/journal.ppat.1002292.
65. **Bisson SA, Page AL, Ganem D.** 2009. A Kaposi's sarcoma-associated herpesvirus protein that forms inhibitory complexes with type I interferon receptor subunits, Jak and STAT proteins, and blocks interferon-mediated signal transduction. J. Virol. **83:**5056–5066. http://dx.doi.org/10.1128/JVI.02516-08.
66. **Madrid AS, Ganem D.** 2012. Kaposi's sarcoma-associated herpesvirus ORF54/dUTPase downregulates a ligand for the NK activating receptor NKp44. J. Virol. **86:**8693–8704. http://dx.doi.org/10.1128/JVI.00252-12.
67. **Barton ES, Lutzke ML, Rochford R, Virgin HW.** 2005. Alpha/beta interferons regulate murine gammaherpesvirus latent gene expression and reactivation from latency. J. Virol. **79:**14149–14160. http://dx.doi.org/10.1128/JVI.79.22.14149-14160.2005.